UNIVERSIDADE DA BEIRA INTERIOR
Ciências da Saúde

Produção de Scaffolds de ß-TCP/Alginato para uso na Regeneração Óssea por Prototipagem Rápida

Gabriela Soares Diogo Carlos

Dissertação para obtenção do grau de mestre em
Ciências Biomédicas
(2º ciclo de estudos)

Orientador: Professor Doutor Ilídio Joaquim Sobreira Correia.

Covilhã, junho 2013

List of publications

Torres, A.L. , Gaspar, V.M. , Serra, I.R. , Diogo, G.S. , Silva, A.P. and Correia, I.J. , Bioactive Hybrid Polymeric-Ceramic 3D Scaffold for Improved Bone Tissue Regeneration. 2013, submitted to *Materials Science and Engineering: C*.

"Que os vossos esforços desafiem as impossibilidades, lembrai-vos de que as grandes coisas do homem foram conquistadas do que parecia impossível"

Charles Chaplin

I would like to dedicate my master thesis to my parents…

Acknowledgments

First, I would like to thank to my supervisor professor Ilídio Correia for the opportunity to develop the theme of my master's thesis with him. For all the dedication and all the time spent in carrying out the whole project.

To Eng. Ana Paula from the Optics center of Universidade da Beira Interior for helping in the acquisition of the scanning electron microscopy images.

To Professor Abílio Silva for all availability to perform the mechanical characterization of the scaffolds.

To all my fellow group colleges. One way or another all contributed to the development of my work. Especially thank to Inês, one of the people who spent more time with me both inside and outside the laboratory. For all the help and understanding throughout this year.

To a very special person who were always by my side, both at personal and professional level, Paulo Machado.

Thank to all my special friends for all its contribution. To Ana Luisa Torres for all the help and support.

A special thank to the most important people in my life, my parents and my siblings for all the support, love, affection and attention. To them I owe my life and my happiness. Special thanks to my best friend, my mother. What I am today, I owe you.

Abstract

The rise of bone defects in the last decades has become a worldwide problem. They can arise from several causes such as tumors, trauma, infection, nutrition and bone diseases. This may compromise the mechanical and biological functions of bone tissue. Autografts, allografts and xenografts are some attractive alternatives used for bone tissue regeneration, however, several factors such as high risk of infection, immunogenic response and lack of donor has limited their use. In this context, Tissue Engineering appears as a promising solution. Tissue Engineering is an interdisciplinary area that combines biomaterials and bioactive molecules to promote the repair and regeneration of bone. Scaffolds are 3D matrices that act as temporary templates, allowing cell adhesion and proliferation and providing mechanical support until new bone tissue formation. A 3D scaffold success depends on their chemical, mechanical and biological properties. Rapid prototyping technologies allow the production of 3D structures with controlled architecture from models created by computer-aided design, through a layer-by-layer process. The present study describes the characterization of the chemical, mechanical and biological properties of ßeta-Tricalcium phosphate/Alginate 3D scaffolds. The scaffolds were characterized by Scanning Electron Microscopy, Fourier Transform Infrared Spectroscopy, X-Ray Diffraction and Water Contact Angle. Porosity and Mechanical properties (Compressive Strength and Young´s Modulus) were also analyzed. The cytotoxic profile was evaluated by *in vitro* MTS assays, using human osteoblastic cells. Confocal Laser Scanning Microscopy was also performed. The results obtained showed that the scaffolds produced by the Rapid Prototyping technique have good chemical and biological properties, which is fundamental for its application on bone tissue regeneration. Furthermore, it is concluded that the scaffolds showed better mechanical and biological properties with the increase of the percentage of ßeta-Tricalcium phosphate within scaffolds.

Keywords

ßeta-Tricalcium Phosphate/Alginate Scaffolds, Bone Regeneration, Computer-Aided Design, Rapid Prototyping, Tissue Engineering.

Resumo

O aumento de defeitos ósseos, nas últimas décadas tem-se tornado um problema de saúde a nível mundial. Estes defeitos têm causas, tais como tumores, traumatismos, infeções, nutrição e doenças ósseas, e podem comprometer as funções mecânicas e biológicas do tecido ósseo. Os autoenxertos, aloenxertos e xenoenxertos são algumas das alternativas utilizadas para a regeneração dos defeitos do tecido ósseo. No entanto, vários factores, tais como, alto risco de infeção, resposta imunogénica no hospedeiro e falta de doadores têm limitado o seu uso. Neste contexto, apareceu a Engenharia de Tecidos como uma área interdisciplinar que combina biomateriais com moléculas bioativas para promover a reparação e regeneração do osso. Nesta área de investigação têm sido produzidas matrizes 3D (scaffolds) que funcionam como modelos temporários, permitindo a adesão e proliferação celular, fornecendo suporte mecânico até á formação de novo tecido ósseo. O sucesso de um scaffold depende das suas propriedades químicas, mecânicas e biológicas. As tecnologias de prototipagem rápida permitem a produção de estruturas 3D com arquitetura controlada, a partir de modelos criados por desenho assistido por computador, através de um processo de camada por camada. O presente estudo descreve a caracterização das propriedades químicas, mecânicas e biológicas dos scaffolds 3D produzidos com ßeta-Tricálcio fosfato/Alginato onde foram usados vários rácios de concentrações de ßeta-Tricálcio fosfato e alginato. Os scaffolds foram caracterizados por Microscopia Eletrónica de Varrimento, Espectroscopia de Infravermelho por Transformada de Fourier, Difração de Raios-X e Angulo de Contato com a Água. A Porosidade e Propriedades Mecânicas foram também estudadas. O perfil citotóxico foi avaliado *in vitro*, através do ensaio de MTS utilizando osteoblastos humanos. Microscopia Confocal Laser foi também realizada de modo a observar a distribuição das células nos scaffolds. Os resultados obtidos mostraram que os scaffolds 3D produzidos pela técnica de Prototipagem Rápida têm boas propriedades químicas e biológicas, o que é fundamental para a sua aplicação na regeneração do tecido ósseo. Além disso, concluiu-se que estas estruturas tridimensionais apresentam melhores propriedades mecânicas e biológicas com o aumento de ßeta-Tricálcio fosfato.

Palavras-Chave

ßeta - Tricálcio fosfato/Alginato Scaffolds, Desenho Assistido por Computador, Engenharia de Tecidos, Prototipagem Rápida, Regeneração Óssea.

Resumo alargado

O osso é um tecido dinâmico e altamente vascularizado com capacidade de auto-regeneração, responsável por muitas das funções do corpo humano. É constituído pela matriz orgânica (maioritariamente colagénio), matriz inorgânica (hidroxiapatite), células (osteoblastos, osteócitos e osteoclastos) e água. No entanto, vários factores, tais como, infeções, doenças e nutrição conduzem á perda das suas funções, nomeadamente perda da capacidade natural de auto-regeneração. Assim, o aumento de defeitos ósseos, nas últimas décadas tem-se tornado um problema de saúde a nível mundial.

Os autoenxertos, aloenxertos e xenoenxertos são algumas das alternativas utilizadas para a regeneração dos defeitos do tecido ósseo, contudo o elevado risco de resposta imunológica por parte do paciente, risco de infeção e rejeição tem limitado o seu uso.

Neste contexto, apareceu a Engenharia de Tecidos como uma área promissora para a resolução deste tipo de problemas. A Engenharia de Tecidos é uma área interdisciplinar que combina biomateriais com moléculas bioativas para promover a reparação e regeneração do osso. O primeiro objetivo da Engenharia de Tecidos passa pela alteração do conceito de substituição pelo conceito de regeneração. Em que matrizes 3D (scaffolds) funcionam como moldes temporários que se degradam á medida que nova matriz óssea é formada.

O sucesso de um scaffold depende de diversos parâmetros, tais como, biocompatibilidade, biodegradabilidade, propriedades de superfície, porosidade e propriedades mecânicas, com o objetivo de promover osteoindução, osteocondução e neovascularização.

Diversos materiais, como metais, polímeros e cerâmicas têm sido utilizados nesta área de investigação. Além disso várias técnicas têm sido utilizadas para produção de estruturas 3D. As tecnologias de prototipagem rápida permitem a produção de estruturas 3D com arquitetura controlada, a partir de modelos criados por desenho assistido por computador, através de um processo de camada por camada.

O presente estudo descreve a caraterização das propriedades químicas, mecânicas e biológicas de scaffolds 3D produzidos com ß-TCP/Alginato. Foram produzidos três tipos de scaffolds diferentes, variando os rácios entre as concentrações de ß-TCP e alginato, scaffolds 50/50 % (w/w), 30/70 % (w/w) e 20/80 % (w/w), respetivamente. Os scaffolds foram produzidos pelo método de prototipagem rápida, recorrendo ao uso de uma impressora 3D chamada Fab@home. O equipamento escolhido para a produção dos scaffolds aplica a técnica de plotting, em que um material simples ou um compósito é extrudido formando os scaffolds.

Os scaffolds foram caraterizados por Microscopia Eletrónica de Varrimento, Espectroscopia de Infravermelho por Transformada de Fourier, Difração de Raios-X e Angulo de Contato com a água. Os resultados obtidos relativamente à caraterização físico-química dos scaffolds permitem concluir que após todo o processo de produção estes não sofrem alterações na sua estrutura cristalina. Além disso, estes apresentam um carater hidrofílico promovendo adesão e proliferação celular. Um dos objetivos na produção de scaffolds é atingir um equilíbrio

entre o grau de porosidade e as suas propriedades mecânicas. Os testes realizados à porosidade e às propriedades mecânicas revelam que os scaffolds 50/50 apresentam melhores condições quando comparados com os grupos de scaffolds 30/70 e 20/80, respetivamente. Por fim, foi feita uma análise *in vitro* ao perfil citotóxico dos scaffolds, através do ensaio de MTS utilizando osteoblastos humanos. Conclui-se que todos os grupos apresentaram boa viabilidade. A viabilidade aumenta com o aumento de ß-TCP. Com o intuito de corroborar o que já foi dito foi feita uma análise de Microscopia Eletrónica de Varrimento e Microscopia Confocal Laser de modo a observar a adesão de osteoblastos e a sua distribuição nos scaffolds. As imagens microscópicas dos scaffolds obtidas pela análise de Microscopia Eletrónica de Varrimento revelaram que os scaffolds apresentam uma superfície rugosa, e ligeiramente regular, assegurando as condições necessárias para que ocorra adesão celular. Tal resultado foi enfatizado quando observadas as mesmas imagens dos scaffolds em contato com as células, as células aparecem aderidas e com uma conformação esticada. Através das imagens de microscopia confocal foi possível observar a distribuição dos osteoblastos no interior dos scaffolds.

Os resultados obtidos mostraram que os scaffolds 3D produzidos pela técnica de Prototipagem Rápida têm boas propriedades químicas e biológicas. Tal é fundamental para a sua aplicação na regeneração do tecido ósseo. Além disso, concluiu-se que estas estruturas tridimensionais apresentam melhores propriedades mecânicas e biológicas com o aumento de ß-TCP. Os resultados sugerem que adição de ß-TCP confere resistência mecânica aos scaffolds e induz o processo de osteogénese.

Table of contents

List of figures

List of tables

Acronyms

3D	Three-Dimensional
3DP	Three-Dimensional Printing
ß-TCP	ßeta-Tricalcium Phosphate
BMP	Bone Morphogenetic Proteins
BSA	Bovine Serum Albumin
BTE	Bone Tissue Engineering
$CaCl_2$	Calcium Chloride
CAD	Computer-Aided Design
CAM	Computer-Aided-Manufacturing
CLSM	Confocal Laser Scanning Microscopy
CT	Computerized Tomography
DMEM-F12	Dulbecco's Modified Eagle's Medium
ECM	Extracellular Matrix
EDS	Energy Dispersive Spectroscopy
EDTA	Ethylenediaminetetraacetic Acid
EtOH	Ethanol
FBS	Fetal Bovine Serum
FDM	Fused Deposition Modeling
FTIR	Fourier-Transform Infrared Spectroscopy
H^+	Hydrogen Ions
HA	Hydroxyapatite
IL-1	Interleukin-1
MSC	Mesenchymal Stem Cells
MTS	3-(4,5-dimethylthiazol-2-yl)-5-(3-carboxymethoxyphenyl)-2-(4-sulfophenyl)-2H-tetrazolium
OB	Osteoblasts
OC	Osteoclasts
PBS	Phosphate-Buffered Saline

PCL	Poly (ε-caprolactone)
PLGA	Poli-lactide-co-glico-lide
PLLA	Poli(L-lactic-acid)
PI	Propidium Iodide
PTH	Paratiroid Hormone
PVA	Poly(vinyl) Alcohol
RANKL	NF-kappa B ligand
RT	Room Temperature
SEM	Scanning Electron Microscopy
SLA	Stereolithography
SLS	Selective Laser Sintering
STL	Stereolithography
TE	Tissue Engineering
TNF	Tumor Necrosis Factor
Ts	Resistance to Compression
XRD	X-Ray Diffraction
YM	Young's Modulus

Chapter I - Introduction

1. Introduction

1. 1. Anatomy and Physiology of Bone

Bone tissue is responsible for the human body support and also by other different biological functions (2-4). Mechanical functions include protection of vital organs and movement, since bones are connected with muscles that when stimulated are responsible for moving the whole body. Biologically, bone tissue is responsible for the production of blood cells, through a process called hematopoiesis, and for the storage of ions, such as phosphorus and calcium (3).

Bone is composed by cells, water and bone matrix. This matrix is formed by organic (35%) and inorganic material (65%) (2, 3). The organic material is constituted by collagen and proteoglycans, while crystals of calcium phosphate, concretely hydroxyapatite (HA) form the inorganic part of this tissue. Both the organic and inorganic compounds of bone tissue are important to maintain flexibility and resistance to compression, respectively (Figure 1a) (2). A decrease in collagen composition contributes for increasing bone fragility and subsequently this tissue can break easily, Figure 1c. On the contrary, if the quantity of bone mineral decreases, bone will bend without breaking, as can be seen in Figure 1b (2).

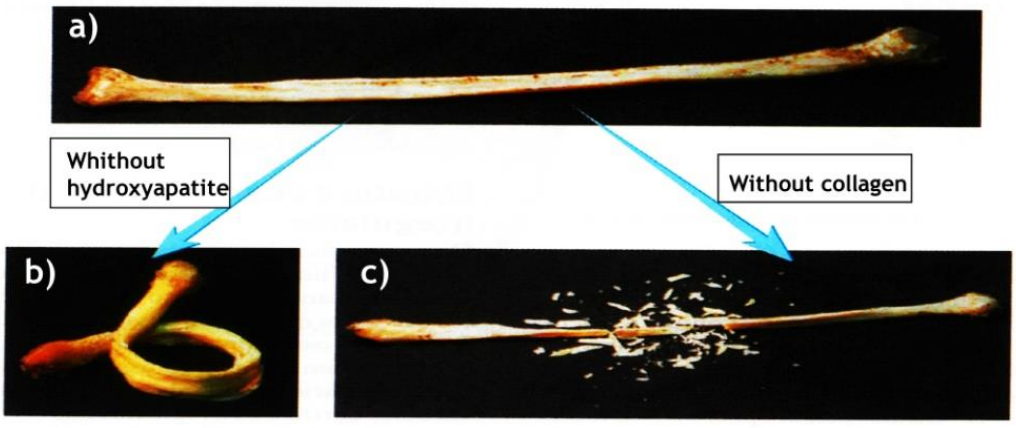

Figure 1 - Bone matrix components. Normal bone a), demineralize bone, without hydroxyapatite b) and mineralized bone, without collagen c) (adapted from(2)).

There are different categories of bone cells, like osteoblasts (OB) (bone-forming cells), osteocytes (bone maintaining cells) and osteoclasts (OC) (bone resorbing cells). Each cell type has different origins and functions, but all of them are equally important to produce new bone matrix (5). Nevertheless, the process of bone formation and regeneration depends on the vascularization system for the transport of nutrients and oxygen, and also for the delivery of circulating osteogenic factores and stem cells (6).

1.1.1. Types of Bone

The human body has several types of bones that can be distinguished according to their shape, surface features and bone matrix. Based on shape, bones can be grouped into four categories: long bones, irregular bones, flat bones and short bones, as presented in Figure 2 (2, 3). Long bones, as their name suggests, have an elongated shape and represent the majority of limb bones, except the patella, wrist and ankle, Figure 2a (3, 4). Irregular bones are named due to their variety of shapes. They present many surface features for muscle or articulation attachment. Examples of this type of bone are the vertebrae and hip bones, Figure 2b (3, 4). Flat bones, have a broad surface that is important for muscle attachment or organs protection, examples are the bones of the shoulder girdle, ribs and breastbone, Figure 2c (3, 4). Finally, Short bones have a roughly cube shape, for instance, the bones of the wrist and ankle, Figure 2d (3, 4).

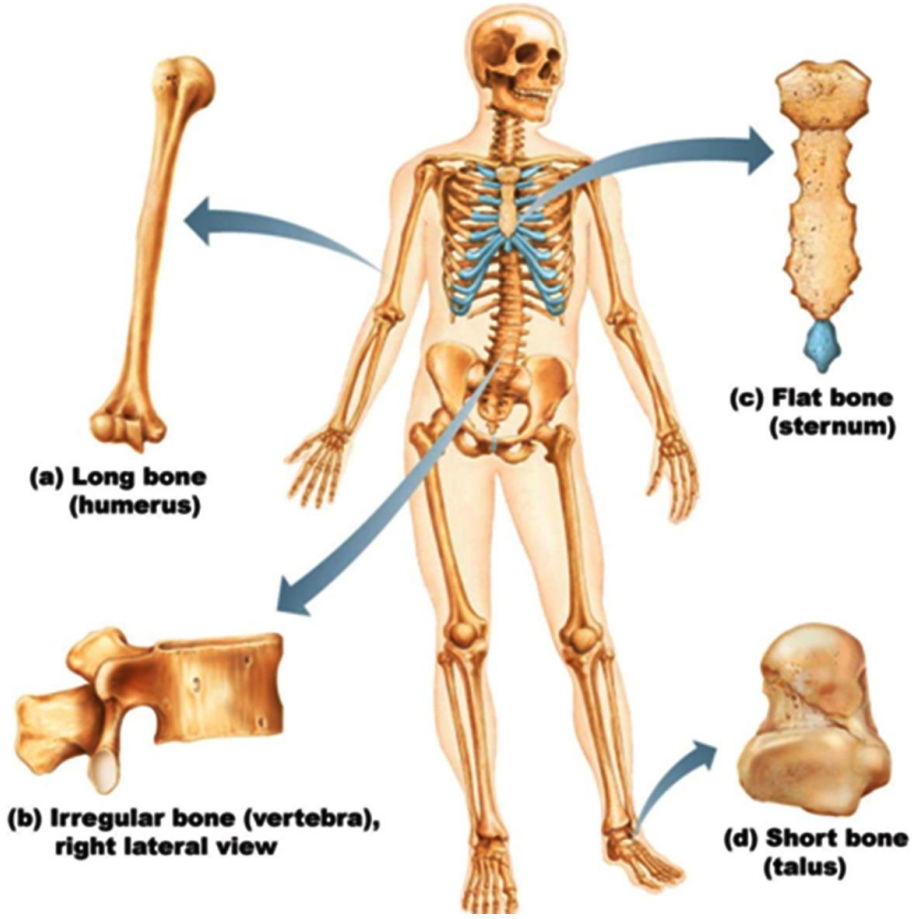

Figure 2 – Representation of the types of bones. According to the shape there are four types of bones: long bones (a), irregular bones (b), flat bones (c) and short bones (d) (adapted from (4)).

Accordingly to the organization of collagen fibers, bone can be classified in reticular and lamellar, whether fibers possess a random or parallel distribution, respectively. Additionally and depending on the density of the bone matrix, bone can be classified in spongy (or trabecular, around 20% of the total skeleton) and compact (or cortical, around 80% of the

total skeleton), as can be seen in Figure 3 (7). The spongy bone has a high porosity (around 50-90%), lower density and lower compressive strength, when compared with the compact type (5, 7, 8).

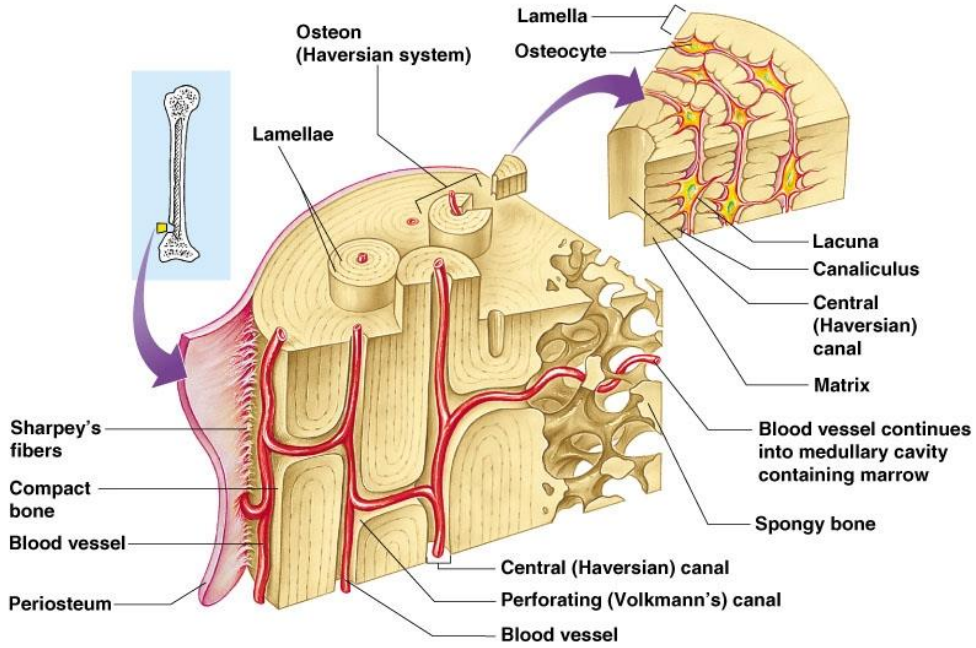

Figure 3 - Representation of the internal structure and organization of bone (adapted from (4)).

1.1.2. Bone Cells

Bone cells, namely OB and OC, have different origins and are responsible for the production and resorption of bone, respectively (9).

OB are mononuclear cells that derive from mesenchymal stem cells (MSC) and are present at bone surfaces (10). These cells present a spherical nucleus, a basophilic cytoplasm, a very developed endoplasmic reticulum and also a large number of ribosomes (11). Structurally they have a cuboid shape or sometimes a slightly elongated appearance, as can be seen in Figure 4. Functionally, OB play an important role in the production of organic matrix, and on its mineralization, being responsible for the production of collagen type I, osteocalcin, osteopontin, osteonectin, proteoglycans and cytokines (8, 11). Furthermore, OB release high levels of alkaline phosphatase, which is normally present on the OB cytoplasmatic membrane, to promote bone mineralization (11).

Moreover, OB possess vesicles that contain phosphate, calcium ions and enzymes, that are released by exocytose and are responsible by hydroxyapatite crystals formation (2). On the other hand, alkaline phosphate and noncollagenous proteins, such as, osteocalcin, osteopontin and bone sialoprotein are important for matrix maturation. It is believed that these calcium and phosphate-binding proteins help in the deposition of mineral by regulation of hydroxyapatite crystals (12). Furthermore, OB also plays an important role in bone

resorption. They promote the contact between OC and the mineralized matrix, followed by the process of re-mineralization (2).

While OB are producing new bone, they became surrounded by bone matrix, leading to their differentiation into osteocytes (2).

Osteocytes are mature cells that have the ability to maintain the bone matrix integrity (2). Osteocytes fill the gaps in the bone matrix and are responsible for intercellular communication (13). They possess cytoplasmatic prolongations called filopodia located in spaces or channels in the bone matrix (13). The arrangement of the canaliculi (Figure 4), allows the passage of nutrients and oxygen between the blood vessels and distant osteocytes (13). Osteocytes are also responsible for osteocytic osteolysis, breaking down the bone matrix for the release of calcium for calcium homeostasis (13).

OC are multinucleated, polymorphic irregularly shaped giant cells, that derive from the hematopoietic lineage, as can be seen in the Figure 4 (2). The OC are the primary cells involved in bone resorption process and are rich in actin and myosin. This is crucial for OC attachment to the bone surface and allows bone resorption to occur in a restricted area (12).

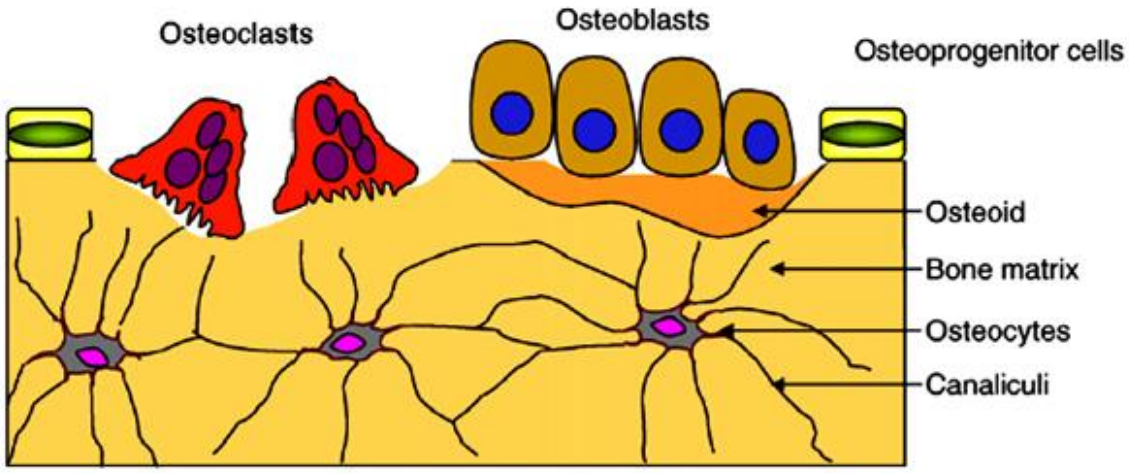

Figure 4 – Schematic representation of the bone. Osteoblasts are involved in bone formation, osteoclasts are involved in bone resorption and osteocytes cells maintain the integrity of bone tissue (adapted from (13)).

1.1.3. Bone Remodeling

Bone is a dynamic and metabolically active tissue that is constantly remodeled. Such process allows the replacement of old bone tissue by new mineralized matrix (2)

Bone remodeling involves two main cell populations, OB and OC, as well as hormones, cytokines and mechanical stimuli. This process occurs in three distinct stages: resorption, reversal and formation stage (Figure 5) (2).

Resorption: Osteoclastic bone resorption involves mineral dissolution and degradation of the organic phase (13). This process depends on the acidic environment and lysosomal enzyme

secretion (13). The acidic environment is crucial for the enzymatic activity of lysosomes and for the activation of metalloproteinases (matrix proteins), that are involved in demineralization of the matrix, contributing for bone degradation (11).

To initiate bone resorption, pre-OC cells migrate towards the bone surface, and attach to the bone matrix, through integrins, present in the cytoplasmic membrane of OC that recognize specific receptors of the bone matrix proteins (14, 15). After OC adhesion to the substrate, the $\alpha_v\beta_3$ integrin promotes the cytoskeletal reorganization, involving the formation of dynamic structures called podosomes (11). Podosomes are important for this attachment and trough their continual assembly and disassembly, they promote OC displacement during the bone resorption process (14). Simultaneously, paratiroid hormone (PTH) stimulates OB to produce proteins, such as collagenase. This enzyme is involved in the degradation of the unmineralized bone matrix and contributes for OC adhesion to the matrix (2). Additionally, an increase in the PTH levels, increases the expression of the receptor of NF-kappa B ligand (RANKL) (1). RANKL will then bind to its receptor on the OC surface, promoting pre-OC maturation, differentiation and activation into OC, leading to bone resorption (Figure 5a) (11). However, when this increase is continuous a decrease in the osteoprogesterin (OPG) protein levels is verified (2). OPG is released by OB and compete with OC by RANKL binding. When PTH increases, OPG decrease and RANKL increase, resulting in an increase of the OC levels (2). Bone resorption depends on the action of OC, namely, secretion of hydrogen ions (H^+) and cathepsin K enzyme (13). H^+ are responsible for acidification and proteolysis of the bone matrix, through enzymes degradation (lysosomal enzymes), whereas cathepsin K degrade all the components of bone matrix, including collagen, at low pH (14, 15). After bone being resorbed by OC, resorption pits are formed on the bone surface (13).

Reversal phase: The process of reversal phase begins and the mononuclear cells appear on the bone surface, as shown in Figure 5b. However, the reversal phase is poorly understood, but it is believed that this phase involves further degradation of collagen and release of growth factores that are fundamental for bone formation initiation (16).

Bone formation: Following this, OB migrate into the areas where bone has been resorbed and start to produce new mineralized matrix, in order to fill the resorption pits (14, 16). First, OB produce osteoid matrix as illustrated in Figure 5b, trough deposition of collagen (16). This is followed by the entrapment of OB within the newly produced matrix and their differentiation into osteocytes (1). OB are also responsible for the production of a variety of growth factors, namely bone morphogenetic proteins (BMP) that play important roles in bone formation (Figure 5c) (1). Finally, in the last osteoid phase, bone formation stops and following bone mineralization, bone lining cells remains in a quiescent state, as it is illustrated in Figure 5d (14).

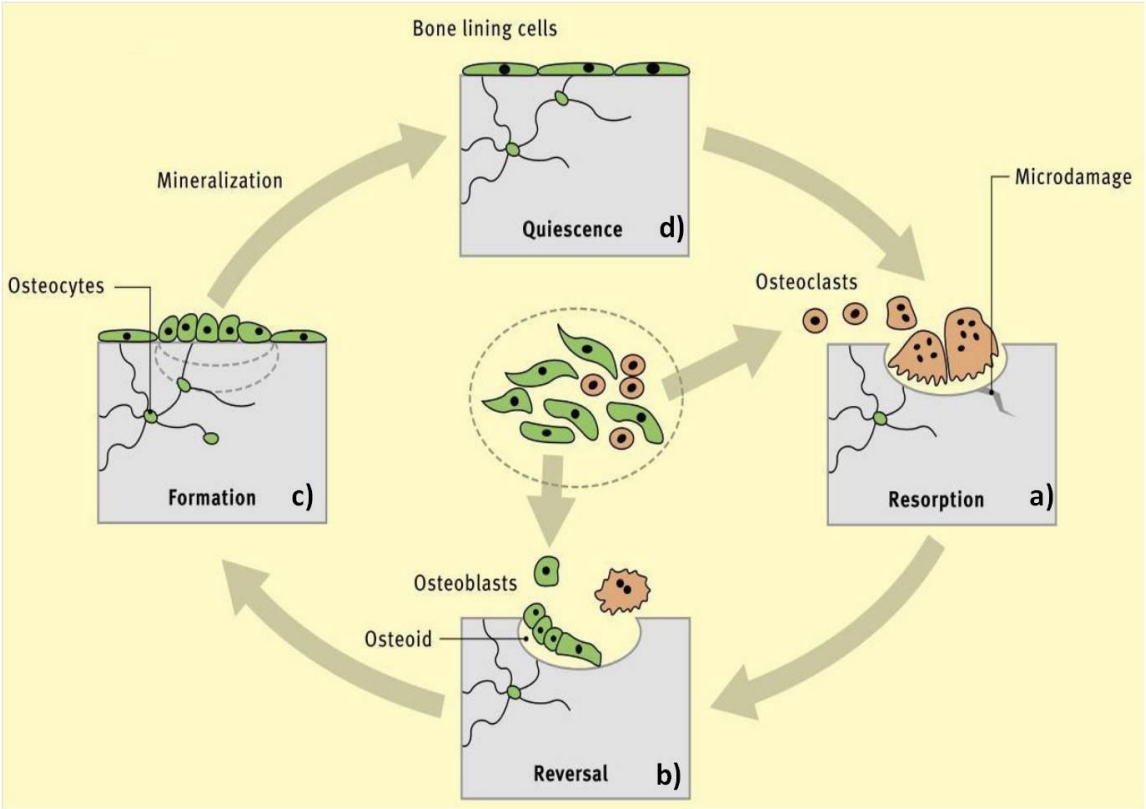

Figure 5 - Schematic representation of the bone remodeling process. To initiate bone resorption (a), pre-OC maturate and differentiate into mononuclear OC, which will merge, originating bigger multinucleated OC that will degrade bone matrix, forming resorption pits. Following this, in the reversal phase (b), OB will migrate towards the degraded areas and will start to produce new mineralized bone. While new bone is being formed by OB in the formation phase (c), OB will get entrapped within the matrix that they are producing, and become differentiated into osteocytes. Finally, bone enters in a quiescent state (d) until a new process of bone remodeling begins (adapted from (1)).

Despite the ability of bone self-remodeling, most diseases that affect bone result from abnormalities in bone remodeling (1). This can compromise the architecture, structure and mechanical strength of bone tissue (1). As a result, clinical symptoms such as pain, deformity, fracture and abnormalities of calcium and phosphate ions homeostasis occur. Biological, mechanical and environmental factors can affect this process (11).

1.2. Bone disorders

As described above, bone is a highly vascularized and mineralized, dynamic and metabolically active tissue, with self-remodeling and healing capacities (17). However, in the last decades the bone defects have been increasing, due to several causes, such as, trauma, tumors, infection or bone diseases (18). A wide-range of diseases and injuries can lead to the loss of the innate capacity of bone to regenerate and lead to loss of function (19). Bony diseases

have three main origins: bone loss in inflammatory diseases, disorders of bone remodeling and monogenic bone diseases (20).

Bone loss in inflammatory diseases are caused by a deregulation of the immune system, i.e., the immune system does not respond properly (20).

Disorders of bone remodeling are related with disparities between the process of resorption and bone formation (15, 20). Examples of disorders of bone remodeling are:

- Osteoporosis that appears when the rate of bone resorption exceeds the rate of bone formation. Osteoporosis increases with age, especially in the women, due to hormonal changes (1).
- Bone metastases occur due to increasing of osteoclastic bone resorption. Osteoclast-activating is stimulated by factors released by tumors cells (e.g. interleukin-1, IL-1 and tumor necrosis factor, TNF) (21).

Monogenic bone diseases are associated with an imperfect process of osteogenesis, which occurs when a lack of control between the levels of collagen products happens (20).

Bone diseases can cause defects in the process of bone remodeling (20).

1.3. Bone Grafts

Nowadays, different therapeutic strategies have been studied to overcome the bone remodeling defects. Treatment options depends not only on the size and location of the defect but also on the patient characteristics, namely, bone quality and age (22). To repair large bone defects, attractive alternatives such as autografts, allografts and xenografts therapies have been used so far in bone tissue reconstruction (18). Bone grafts are the most commonly transplanted tissue after blood transplants (23).

Autografts are bone grafts, in which the bone is obtained from another part of the patient's body (7, 18). Nowadays, autografts are the most commonly used grafts for bone tissue regeneration (22). They have osteoconductive, osteioconductive, and osteogenic properties (18, 23). The major problem in the use of autografts is the limited supply by donor (18). Frequently the size of the bone defect is larger than the area of the tissue obtained for transplantation (18). Furthermore, the use of autografts is limited, by a considerable donor site morbidity, which increases with the amount of harvested bone. Harvesting can induce bleeding, hematoma, infection and chronic pain for patient (22).

To overcome the lack of donor tissue, allografts have also been applied. However, since the grafts are from different donors (of the same species), there is always a risk of disease transmission and of triggering of an immune response from the host (7, 18, 22).

Xenografts are grafts obtained from organisms of different species, which increases the probability of graft rejection by the host (22).

As an alternative to these bone substitutes, different biomaterials (ceramics, polymers and composite systems) have been studied for scaffolds production. The purpose of using scaffolds is not to replace the bone but create temporary matrices for bone growth.

1.4. Bone Tissue Engineering

As previously described, the aging of the population and bone disorders have as consequence a decrease in the bone remodeling and regeneration capacity (1). In these cases, it is indispensable the use of substitutes that replace the function of the damaged or degraded bony tissues due to the limitations associated with autografts, allografts and xenografts in bone tissue regeneration (18, 23). Tissue Engineering (TE) appears has a promising solution to overcome these limitations. TE is "an interdisciplinary field of research that applies the principles of engineering and life sciences, that have contributed for the development of biological substitutes to restore, maintain, or improve tissue function", i.e, TE is a new multidisciplinary field that involves the use of scientific knowledge to solve practical and clinical problems (7).

A primary objective of TE is changing practical practice, addressing the lack of donors and organ rejection (24). In the last years, healthcare has been changing its replacement concepts to a regeneration concept, trough TE and regenerative medicine (25).

The combination of TE and regenerative medicine promotes the development of techniques for the treatment of bone defects (19).

TE approaches have been developed to create new different therapeutics for bone defects regeneration. Which include drug delivery systems and scaffolds, among others, to promote the regeneration of bone without causing adverse effects on the patient (26).

1.4.1. The importance of 3D Scaffolds for Bone Regeneration

Several types of biomaterials, are being used to produce injectable substances, hydrogels and three-dimensional (3D) scaffolds to be applied in bone regeneration (27). Specifically, the design of 3D porous scaffolds is being extensively explored in order to produce 3D structures that allow tissue and organs regeneration (28).

Scaffolds are porous 3D matrices that act as temporary templates, allowing cell adhesion and proliferation, and providing mechanical support until new bone tissue is formed at the defect site (14).

The successful of a 3D scaffold depends on several parameters, such as biocompatibility, biodegradability, surface properties, porosity and mechanical properties, in order to induce osteoinductivity, osteoconductivity of bone-producing cells and neovascularization (6, 18). Osteoinduction is the ability of a scaffold to induce non-differentiated stem cells, or

osteoprogenitor cells from the surrounding tissue, to differentiate into bone-forming OB (18). Considering the importance of OB for the production of new bone matrix, it is essential that the scaffolds have good osteoinductive properties. Osteoconduction is characterized as the ability of osteogenic cells to migrate into the surface of the scaffold and then promote the formation of new blood vessels (18). Neovascularization is the formation of new blood vessels from existing blood vessels to restore the blood supply, helping bone regeneration, during the fracture healing process (6).

Biocompatibility: A biomaterial can be classified as biocompatible whether, when in contact with any tissue it do not causes any immune reaction by the host (29). The biocompatibility depends on the material variables (e.g. surface topography, surface charge), the location of the injury in the body, age, genre, general health, lifestyle features and the presence or absence of microorganisms at the site of implantation (29).

Biodegradability: Scaffolds must be composed by biodegradable materials (30, 31). The rate of degradation of scaffolds must be accompanying the rate of regeneration of new bone (7, 32). As a result a scaffold must be completely degraded when the injury site is totally regenerated (7). Moreover, the rate of scaffolds degradation depends on the extent and site of the injury, as well as on the biomaterial and on the technique applied for its production (7).

Surface properties: Also important are the materials surface properties (30). Among them are the hydrophobic/hydrophilic character, charge, roughness, softness and chemical composition of the biomaterials (30). Surface modifications of biomaterials allow a greater understanding and control of the materials characteristics (33). These surface properties should be controlled in order to induce osteoinductivity, osteocondutivity and osteointegration (18). These properties have an essential role on cellular response, namely, morphology, attachment, differentiation and proliferation of cells (30).

Porosity, pore size and mechanical properties: These properties are important requirements to obtain optimized scaffolds for tissue regeneration (33). The use of ordered structures is essential to achieve a better control of these properties that can influence cells behavior (18). Scaffolds must possess pores with inter-connectivity among them, in order to ensuring the nutrients and oxygen exchange within the scaffold to maintain cell viability and bone regeneration (30, 31). The porosity of the native bone is approximately 10% for the cortical bone and between 50 to 90% for the trabecular bone (7). It is also well accepted that materials ideal pore size for bone tissue engineering should be in the range between 200 μm-900 μm (7). The pores size must be adequate in order to not compromise both the biological functions and the mechanical stability (7). Pores with adequate size allow cells to migrate and attach to the surface of a material, but interconnected pores are essential for cell

growth within the scaffold (30). Mechanical properties of human bones vary accordingly to the type of bone. Cortical bone has a compressive strength of 100-230 MPa and cancellous bone has a compressive strength of 2-12 MPa (7, 34). The Young´s modulus of cortical bone varies between 7-30 GPa and for cancellous bone it varies between 0.5-0.05 GPa (34). Thus, an ideal scaffold should combine good biological properties with good mechanical properties (31). They must have sufficient mechanical strength to support the region to be repaired (7). This is important to stand hydrostatic pressures and to maintain the spaces needed for cell growth and new matrix formation (7).

1.4.2. Materials used for Scaffolds Production

Metals, ceramics and polymers are the most commonly used materials in TE for the production of scaffolds aimed for bone tissue regeneration (18). Despite of its high mechanical strength, the use of metals for bone regeneration has been decreasing due to poor and incomplete osteointegration with surrounding bone (18). So, ceramics and polymers have been studied for being applied in TE (18). Ceramics have been used due to their intrinsic excellent biocompatibility and bioactivity, which means that they are able to promote cell adhesion, proliferation and differentiation (35). Hydroxyapatite (HA) is the major inorganic component of bone and it is usually the first option for scaffold production to be used in bone regeneration (36). However, HA has the disadvantage of having low biodegradability (26). Conversely, ß-Tricalcium phosphate (ß-TCP) has been used for the production of scaffolds, since it revealed better bone formation and degradation rate than HA (36, 37). Furthermore, ß-TCP is an interesting ceramic material studied to be applied in bone tissue regeneration due to their osteocondutivity and osteoinductivity, contributing for bone formation through induction of OB differentiation (38). Due to high biocompatibility, calcium phosphate ceramics are also applied as carrier materials for cell adhesion and growth (35). However, ß-TCP presents also some limitations, like brittleness and poor resistance to fatigue (18).

The combination of ceramics with polymers can provide 3D structures with good bioactivity, adequate mechanical properties and stability (18). Nowadays, there are several types of polymers that can be divided in two different groups: natural polymers (e.g collagen, chitosan, fibrin, alginate) and synthetic polymers (e.g PCL Poly (ε-caprolactone), PLLA poli(L-lactic-acid), PLGA (poli-lactide-co-glico-lide)). Thus, synthetic or natural polymers have been used to improve the bioceramics mechanical properties (7, 18). Natural polymers have high biocompatibility and lower immunogenic risk (7). They exhibit good osteocondutive properties with a high capacity to interact with host´s tissues. However the use of these natural polymers is limited due to their low mechanical stability. On the other hand, the mechanical properties of synthetic polymers can be controlled (7).

Alginate is a natural polysaccharide extracted from brown seaweeds (26, 39). This polymer is composed by 1,4-linked ß-D-mannuronic acid (M) and α-L-guluronic acid (G) residues and has

affinity for divalent cations such as, Ca^{2+}, Sr^{2+} and Ba^{2+} (Figure 6). Through ionic interaction between the cation and the carboxyl functional groups of the G units of alginate, stable hydrogels can be formed (26). This makes alginate a suitable candidate for Bone Tissue Engineering (BTE) applications. Furthermore, it can be used to produce different structures, such as fibers, nanofibers, nanoparticles and microparticles (39). Physiologically, alginate is biocompatibility and does not represent any immunologic risk, ensuring cell viability (39). Additionally, alginate mechanical properties are also attractive, due to their stiffness, elasticity, surface topography and degradability (39). Besides this properties, alginate have been applied for bone regeneration to guide tissue repair, since it provides a biomimetic temporary extracellular matrix (ECM) for cells to infiltrate and migrate while the depositing of new bone tissue occur (39)

However, the properties of the alginate gels (stiffness, elasticity and stability) are highly sensitive to the species and concentrations of ions present in solution (40). Alginate with high content of G residues gives stiff and stable gels, whereas alginate with a low content of G residues results in more elastic and less stable gels (39).

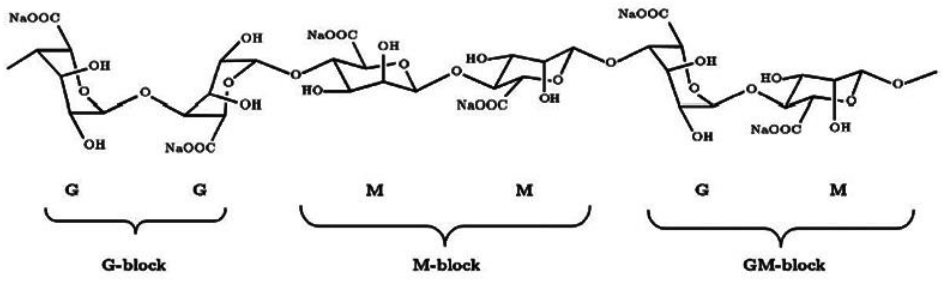

Figure 6 - Chemical structure of sodium alginate (adapted from (41)).

1.4.3. Production of 3D Scaffolds by Rapid Prototyping Technique

Rapid prototyping technologies allow the production of structures in a short period of time, from models created by computer-aided design (CAD) (42). All Rapid prototyping technologies are based on the same principle, construction of 3D models through a layer by layer process (43). This layer by layer process is repeated until the 3D structure is completed (24).

The number of scientific papers and patents based on the RP process, has been increasing over the last several years (42). RP technique can be used in different fields (Figure 7) and when associated with tissue engineering, it can be applied for the regeneration of different tissues such as, bladder, bone, cartilage, heart valves, liver, muscle, nerves, among others (24, 42).

In recent years, the applications of rapid prototyping techniques in the biomedical field have been increasing. The biomedical field represent 15% of the total applications of RP technologies, as can be seen in Figure 7 (42). The development of anatomical models was one of the first factors that helped introduce RP technologies into the biomedical field (42).

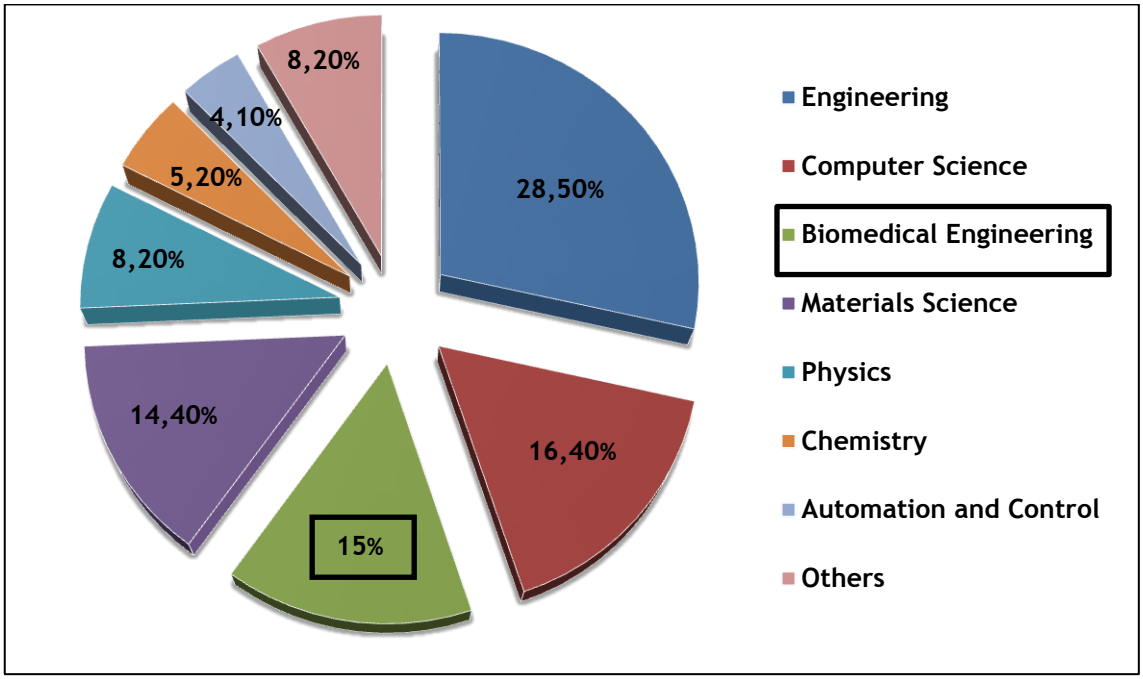

Figure 7 - Rapid Prototyping technology applications (adapted from [38]). Impact of Rapid Prototyping in Biomedical applications.

RP technologies have been used for 3D scaffolds production to be applied in bone tissue regeneration in order to overcome the limitation of conventional fabrication methods (44). RP technique has more advantages than conventional or manual-based fabrication. The possibility to design the architecture of scaffolds with a well-defined 3D structure and control the pore size and porosity with a high degree of reproducibility, makes RP a promising alternative to classical methods of scaffolds production (45).

Moreover, RP, when combined with imaging techniques like CT (computerized tomography) scans, allows the creation of patient specific anatomical parts (44). Using image acquisition technologies, such as computerized tomography (CT) or Magnetic Ressonace Imaging (MRI), it is possible to create an accurate 3D anatomic model of the tissue (36). Based on the data collected in daily routine clinic examinations and computer-aided-manufacturing (CAM) programs, a 3D volume of the tissue can be rendered and then used in the production of a patient specific physical model through RP techniques (36). Furthermore, it promotes a desired level of complexity into the scaffold that can not be achieved with conventional and manual manufacturing techniques (46).

Controlling these parameters allow the production of scaffolds with improved mechanical and biological properties to improve cell adhesion, proliferation and osteogenic differentiation

(44). As previously described in section 1.4.1, these properties of scaffolds play a key role in the process of bone regeneration.

RP techniques: RP techniques involve for example stereolithography (SLA), selective laser sintering (SLS), fused deposition modeling (FDM), three-dimensional printing (3DP) and 3D plotting (47). SLA uses the capacity of some polymers to suffer photo polymerization (in which liquid polymers solidify when exposed to a ultraviolet light) (21). In SLS, a laser beam is focused on a polymer powder and raises the temperature of the powders, causing the fusion of the particles (7). Another RP technique is FDM, which uses a small temperature-controlled extruded material and deposit simultaneously polymer onto a platform and constructs a 3D structure through a layer-by-layer process (46). 3D printing, employs inkjet for powders materials and a printer head to print a liquid binder to form a layer by layer scaffold (7).
3D Plotting was described for the first time by Landers et al. (24). Briefly, 3D plotting is a system based on a dispenser solution that is forced to pass through a syringe onto a platform to generally form a hydrogel. For this, a dispenser solution must fall onto a crosslink agent (7). One of the newer techniques in 3D plotting consists in the fabrication technology based on the extrusion of continuous filaments (48).
In this work, a 3D printer called Fab@Home was used for scaffolds production. Fab@Home was developed by Cohen and collaborators, and they applied the plotting technology for scaffold production (48).

1.4.3.1. Fab@Home Model for Scaffolds Production

There are several machines that can be used for RP. However, the majority of the commercially available machines are not suitable for biomedical purposes, like bone regeneration. Fab@home is one of the available machines that can be applied in bone 3D structures production (42, 49).
The Fab@home model has advantages over other equipments, since it allows the employment of different samples, such as composite materials and viscous solutions, like hydrogels (49). However, the printing accuracy and resolution of the extruded material depends on a set of factors, such as material viscosity, dispensing pressure, pushout (specifies the initiate material-flow before the cartridge moves along the print path), suckback (sets how long the syringe plunger with draws at the end of the path to stop the extrusion), nozzle diameter, deposition rate, printspeed, pathheight (distance between adjacent layers) and pathspace (distance between adjacent paths for each layer), (Figure 8) (50).

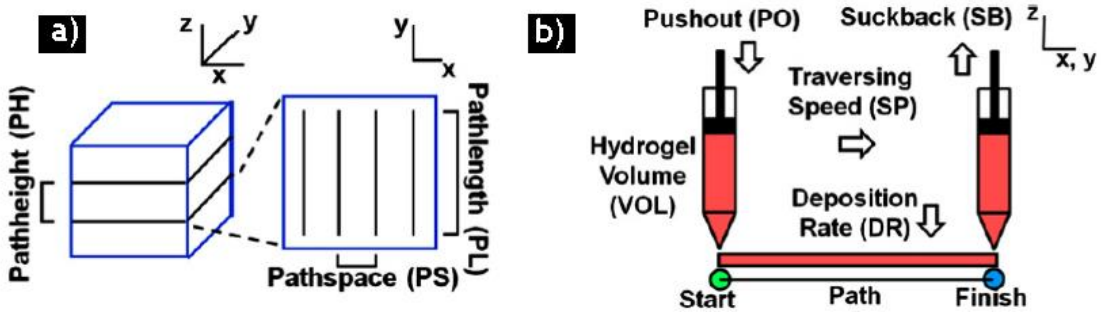

Figure 8 - Representation of the various parameters used for the extrusion of the composite material. Parameters controlling the path generation a) and parameters controlling material extrusion b). (adapted from [46]).

The RP process begins when an object is scanned or designed in a CAD. CAD allow the design of models of various geometries (48). Then the CAD files are converted in a STL format. (51) After, the syringe is loaded with the material solution, followed by the set up of specific parameters. Finally, the solution is extruded onto a platform and the scaffolds are produced (Figure 9).

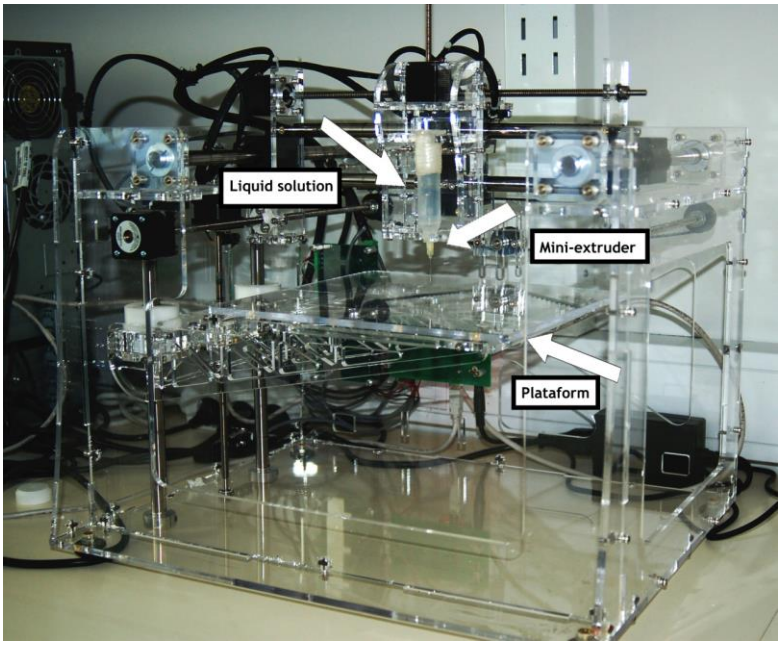

Figure 9 - Fab@home photograph used to produce 3D scaffolds for bone regeneration.

1.5. Aims

Production of ß-TCP/Alginate composites scaffolds by Rapid Prototyping for bone regeneration.

- Design optimization of 3D structure using Solidworks software;
- Optimization of the viscosity of the solution to extrude;
- Study of the influence on the variation of the ratios between the ß-TCP and alginate scaffolds properties;
- Evaluate the mechanical, physicochemical and biological properties of the produced scaffolds.

Chapter II - Materials and Methods

2.1 Materials

Amphotericin B, bovine serum albumin (BSA), cacodylate (Mw=214.03 g/mol) buffer, calcium chloride ($CaCl_2$) (Mw=110.98g/mol) solution, dulbecco's modified eagle's medium (DMEM-F12), Ethanol (EtOH), ethylenediaminetetraacetic acid (EDTA), 2.5 % (v/v) glutharaldehyde, L-glutamine, penicillin G, phosphate-buffered saline (PBS), poly(vinyl) alcohol (PVA) (Mw=31 000g/mol), sodium alginate solution (Mw=120.000 – 190.000 Da), streptomycin, trypan blue, trypsin were purchased from Sigma-Aldrich (Sintra, Portugal). ß-TCP powder, molecular weight (Mw=310,20g/mol) was purchased from Panreac® (Barcelona,Spain). 3-(4,5-dimethylthiazol-2-yl)-5-(3-carboxymethoxyphenyl)-2-(4-sulfophenyl)-2H-tetrazolium reagent, inner salt (MTS) was obtained from Promega (Madison, USA). Fetal bovine serum (FBS) was purchased from Biochrom AG (Berlin, Germany). Human osteoblast cells (CRL-11372) were purchased from American Type Culture Collection (VA, USA). 96-well plates were acquired from Orange Scientific (Braine LÁlleud, Belgium). µ-Slide 8 well Ibidi® chamber coverslips (Ibidi® GmbH, Germany). Propidium Iodide was purchased from Invitrogen (Carlsbad, USA).

2.2 Methods

2.2.1. Preparation of ß-TCP/Alginate Composite Scaffolds by Rapid Prototyping.

The bioactive 3D scaffolds were produced by the RP technique. This technique allows the production of scaffolds with controllable porosity, well-defined 3D microstructures and greater reproducibility (47). A Fab@home printing model was used for scaffolds production, since the scaffolds architecture produced with 3D plotters can be controlled trough a computer-assisted designed. Such is fundamental for allowing the manipulation of 3D models that are capable of sustaining cellular viability (45).

First, alginate and ß-TCP solutions were prepared. Briefly, to prepare alginate solution, alginate was dissolved in milli-Q water. Then, the solution was left overnight under magnetic stirring, and then sonicated for 15 minutes to homogenize the mixture. Following, ß-TCP powder was weighed and added to the alginate solution.

In this study, three different types of scaffolds were produced, varying the ratios between the concentrations of ß-TCP and alginate. ß-TCP/Alginate scaffolds were produced using solutions prepared with ß-TCP and alginate in a proportion of 50/50 % (w/w), 30/70 % (w/w) and 20/80 % (w/w), respectively. For that, PVA (ß-TCP binder agent) was added to the polymer-bioceramic mixture in a ratio of 1:10 (% w/w) PVA:ß-TCP.

After the dissolution of all components, a 1% $CaCl_2$ solution was added to the polymer-bioceramic mixture, in a ratio of 1:2 (% V/V) $CaCl_2$: alginate. This is an important step, since $CaCl_2$ allows the formation of a hydrogel, through a reticulation process, controlling the extrusion during the scaffolds production (49).

Scaffolds were designed in a computer program called Solidworks. This software allows the creation of 3D models with a controllable structure. To initialize the printing of the scaffolds the files were converted and stored in stereolithography (STL) formats. Herein a layer-by-layer fabrication process was used to produce the 3D model. Finally, the solution was filled into a syringe and extruded through a nozzle. The scaffolds were then immersed in a 5 % $CaCl_2$ solution, in order to crosslink them, and maintained there for 24 hours. Then, the scaffolds were frozen at -80ºC and subsequently lyophilized for 24 hours, in order to allow their drying.

Table 1 – Composition of the ß-TCP/ Alginate scaffolds produced.

Scaffolds	ß-TCP	Alginate	PVA
50/50	50%	50%	1:10 (% w/w) PVA:ß-TCP
30/70	30%	70%	1:10 (% w/w) PVA:ß-TCP
20/80	20%	80%	1:10 (% w/w) PVA:ß-TCP

2.3 Morphological and Physicochemical Characterization of Scaffolds

2.3.1. Scanning Electron Microscopy analysis

In order to evaluate scaffolds morphology, porosity and cellular behavior in the presence of the scaffolds, Scanning Electron Microscopy (SEM) analysis was performed following the method adapted from Valente *et al.* (26). Samples were washed at room temperature with cacodylate buffer solution and fixed for 30 min with 2.5 % (v/v) glutharaldehyde diluted in a 0.1 M sodium cacodylate solution. Then, samples were washed three times with cacodylate buffer and finally incubated for 10 min in a graded series of ethanol solutions (50, 60, 70, 80, 90 and 99 % v/v), for dehydration. Scaffolds were then stored in absolute ethanol, at 4 ºC, until being subjected to CO_2 critical point drying, mounted onto aluminum stubs with Araldite glue and sputtered-coated with gold using an Emitech K550 sputter coater. SEM images were obtained with a scanning electron microscope Hitachi S-2700 (Tokyo, Japan) with an

acceleration voltage of 20 kV at suitable magnifications.

2.3.2. Fourier Transform Infrared Spectroscopy analysis

Fourier-transform infrared (FTIR) spectroscopy was used to measure the physicochemical characteristics of the scaffolds and the chemical cross-linking of different compounds (26). FTIR spectra represent the average of 128 scans between 400 and 4000 cm^{-1}, at a resolution of 4 cm^{-1}. Briefly, all samples were crushed and the resulting powders were mounted on a diamond window and recorded on a Fourier-transform infrared spectrophotometer (Nicolet iS10), from Thermo Scientific, (Waltham, MA, USA). β-TCP and Alginate powders were also analyzed to perform a comparative study with scaffolds samples (45).

2.3.3. X-Ray Diffraction analysis

To evaluate the characteristic phases and crystallinity of the scaffolds after being produced, X-ray diffractometry measurements were performed with a diffractometer (Rigaku Americas Corporation, USA) (52). XRD technique was used to examine material composition after the process of freezing and lyophilization to confirm the presence of β-TCP and Alginate in the scaffolds. Samples were mounted in appropriate silica supports and the data was recorded over a range of 5 ° to 90 ° 2θ degrees, with continuous scans at a rate of 1°/min with a copper ray tube operated at 30 kV and 20 mA (53).

2.3.4. Energy Dispersive Spectroscopy analysis

In order to perform the elementary characterization of the materials, in this specific case to evaluate the distribution of elemental calcium and phosphorus in the scaffolds, an energy-dispersive spectroscopy (EDS) (Rontec) analysis was carried out. For that, samples were placed on an aluminum stub support, air-dried at room temperature (RT) and sputter-coated with gold (53).

2.4. Mechanical Characterization of the β-TCP/Alginate Composite Scaffolds: Resistance to Compression and Young's Modulus.

In order to study the mechanical behavior of the scaffolds, compression assays were performed by following a method adapted from Santos *et al*. (36). First, the previously

lyophilized scaffolds were cut into similar sizes fragments and their dimensions determined. The compression assays were performed using a Zwick® 1435 Material prüfung (Ulm, Germany) with a crosshead speed of 0.2 mm /min and a load cell of 5 kN. Five specimens from each sample were tested and their dimensions acquired. The calculation of the resistance to compression (Ts) of each scaffold was determined through equation 1 (54).

$$Ts = \frac{\mathrm{F}}{a \times l} \qquad (1)$$

Where *F* is the load at the time of the fracture and *a* and *l* represent the width and length of the scaffold, respectively. Young's Modulus (YM) was obtained from the stress-strain relations calculated and applying the equation 2 (55).

$$YM = \frac{Ts}{Hd} \qquad (2)$$

Where *Hd* is the scaffold height deformation and *Ts* is the scaffold tensile strength. Average values and standard deviations (s.d.) were determined for each sample (*n*=3).

2.5. Contact Angle Measurements

The contact angle measurements of the samples were performed using the sessile drop technique using water as a reference fluid. The method used was adapted from Correia *et al*. (56). Contact angle data was acquired in a *Data Physics Contact Angle System OCAH 200* apparatus, operating in static mode at RT. For each sample, water drops were placed at various locations of the analyzed surface [47].

2.6. Porosity Evaluation

The total porosity (P) of the different types of ß-TCP/Alginate scaffolds was determined by following a method adapted from Nie *et al*. (57). The total amount of absolute ethanol (EtOH) that the scaffolds were able to absorb in 48 h, was determined by applying the equation 3, adapted from Correia et al. (56).

$$P(\%) = \frac{\mathrm{w2-w1}}{\mathrm{d\ ethanol} \times \mathrm{V\ scaffold}} \times 100 \qquad (3)$$

Where W_1 and W_2 is the weight of the dry and the wet scaffold, respectively, $d_{ethanol}$ is the density of the ethanol at RT and $V_{scaffold}$ is the volume of the wet scaffold, directly determined by immersion. For each scaffold, three replicates were analyzed and data represents the average of each replicate.

2.7. Biological Characterization of the ß-TCP/Alginate Composite Scaffolds

2.7.1. Cell Culture and Seeding in the ß-TCP/Alginate Scaffolds

Human Osteoblasts (CRL-11372), were cultured in Dulbecco's modified Eagle medium (DMEM-F12), containing 10% of heat inactivated fetal bovine serum (FBS), streptomycin (100 µg /mL) and gentamicin (100 µg /mL) antibiotics, in a 75 cm^2 T-flasks. Cultures were maintained in a humidified environment at 37ºC, with 5% CO_2, until confluence was attained. After that, cells were trypsinized with 0.18 % trypsin (1:250) and 5 mM EDTA, centrifuged at 260rpm for 5 minutes and the resulting pellet resuspended into 5 mL of complete culture medium. After that, the cellular density (number of cells per mL) was determined by using the trypan blue method. Cells were counted in a Neubauer Chamber and the total number of cells determined accordingly to equation 4:

$$\text{Total cell number} = \frac{\text{counted cells}}{4} \times \text{dilution factor} \times 10^4 \qquad (4)$$

Prior to cell being seeded in contact with scaffolds, they were cut into the desired size and placed into 96-well plates for sterilization and disinfection. Briefly, scaffolds were disinfected with 70% of EtOH solution for 30 minutes and then washed with DMEM-F12 medium twice, followed by sterilization with ultraviolet (UV) light for another 30 minutes. The scaffolds were previously equilibrated with complete culture medium at 37 ºC, for 24 hours. Finally, cells were seeded at scaffolds surface with a density of $10x10^3$ cells per well, to evaluated cell viability and proliferation at days 1 and 7 respectively. The culture medium was changed every two days until day 7.

2.7.2. Evaluation of Cell Viability in the Presence of the Scaffolds.

To evaluate cell viability in the presence of the materials, Human Osteoblasts (CRL-11372) cells were seeded in the presence of the materials in 96-well plates at a density of $10x10^{3,}$

cells per well. Cell viability was determined using a MTS assay at 1 and 7 days after seeding. After an incubation of 24h, the metabolic activity of cells was evaluated by quantifying the metabolic reduction of the MTS to formazan. Briefly, the medium of each well was removed and the cells in contact with scaffolds were incubated with a mixture of 100µL of fresh culture medium and 20µL of MTS/PMS reagent solution, for 4 hours, at 37 ºC. After 4 hours of incubation, 80 µL of the supernatant was transferred into a 96-well microplate and the fluorescence intensity was measured at 492 nm using a microplate reader (Sanofi, Diagnostics Pauster).

Five replicates of each sample were used for each incubation day. Cells cultured without materials were used as negative controls (K^-) and cells cultured with EtOH (96%) were used as a positive control (K^+).

2.7.3. Analysis of 3D Scaffolds Biologic Properties

The analysis of osteoblasts adhesion and morphology on the 3D scaffolds surfaces was visualized by Confocal Laser Scanning Microscopy (CLSM). Briefly, 4 days after seeding cells, the culture medium was removed and cells washed three times with cacodylate buffer at room temperature (RT). The remaining cells were then fixed with cacodylate buffer for 30 min, at RT. Afterwards, the cell nucleus was labeled with Propidium Iodide (PI) solution, during 15 min, at RT, followed by 6 additional washes with cacodylate buffer. The cell-seeded scaffolds were then transferred into µ-Slide 8 well Ibidi® chamber coverslips and imaged in a Zeiss LSM 710 confocal microscope (Carl Zeiss SMT Inc., USA) equipped with a Plan-Neofluar 10x/NA 0.3. All data was acquired in z-stack mode with a step of 4.67 µm. Z-stacks were then rendered into 3D images in the Zeiss Zen software. Depth code rendering of z-stacks was also performed in Zeiss software with the open GL and transparent rendering mode to provide visualization of cell spatial distribution within the scaffold architecture.

2.8. Statistical Analysis

Comparison of the results obtained for the different groups of scaffolds at various conditions was performed by using one-way analysis of variance (ANOVA), with the Newman-Keuls test. A *p* value less than 0.05 ($p<0.05$) was considered statistically significant.

Chapter III - Results and Discussion

3.1. Morphology and Macroscopic Properties of the Scaffolds.

The scaffolds used for bone tissue regeneration must possess, among other properties, adequate external and internal structures, biodegradability during bone tissue growth and their mechanical strength should be sustained during this process (45).

Alginate was chosen based on its biocompatibility and the capacity to act as a temporary replacement of ECM for bone tissue repair ensuring the essential biological properties for cell infiltration and migration while new bone tissue deposition occur (39). The ß-TCP ceramic was chosen based on its intrinsic biocompatibility, osteocondutivity and osteoinductivity and the ability to increase the mechanical properties of alginate (39).

In this study, scaffolds with controlled architecture and porosity were produced by RP technology, as can be seen in Figure 10.

Macroscopic images were acquired in order to characterize the morphologic properties of 50/50, 30/70 and 20/20 scaffolds. It is possible to observe that despite using the same manufacturing process for all scaffolds, the images obtained revealed some differences between scaffolds, as can be observed Figure 10.

Observing the panorama of the different scaffolds, it is possible to verify that the 50/50 scaffolds (Figure 10A) have a more well-defined structure than the 30/70 and 20/80 scaffolds (Figure 10 B,C). This result may be related to the fact that the 30/70 and 20/80 scaffolds had a higher concentration of alginate. According to what was previously described in the literature, the major disadvantage of the alginate is that its reticulation rate is too fast and hard to control, which results in structures that are not always uniform, as noted in Figure 10C (58). The 50/50 scaffolds have lower concentration of alginate and higher concentration of ß-TCP when compared to 30/70 and 20/80 scaffolds. These 50/50 scaffolds showed a better defined structure, as it is possible to observe in Figure 10A.

Moreover, it is possible to observe the presence of microporosity in the 50/50 and 30/70 scaffolds, Figure 10 (D,E) and a lower microporosity on 20/80 scaffolds (Figure 10F). Based on the results it is possible to conclude that the 50/50 and 30/70 scaffolds have a larger surface area, which is fundamental to allow better protein and cell adhesion and also allow capillary in-growth (7, 59).

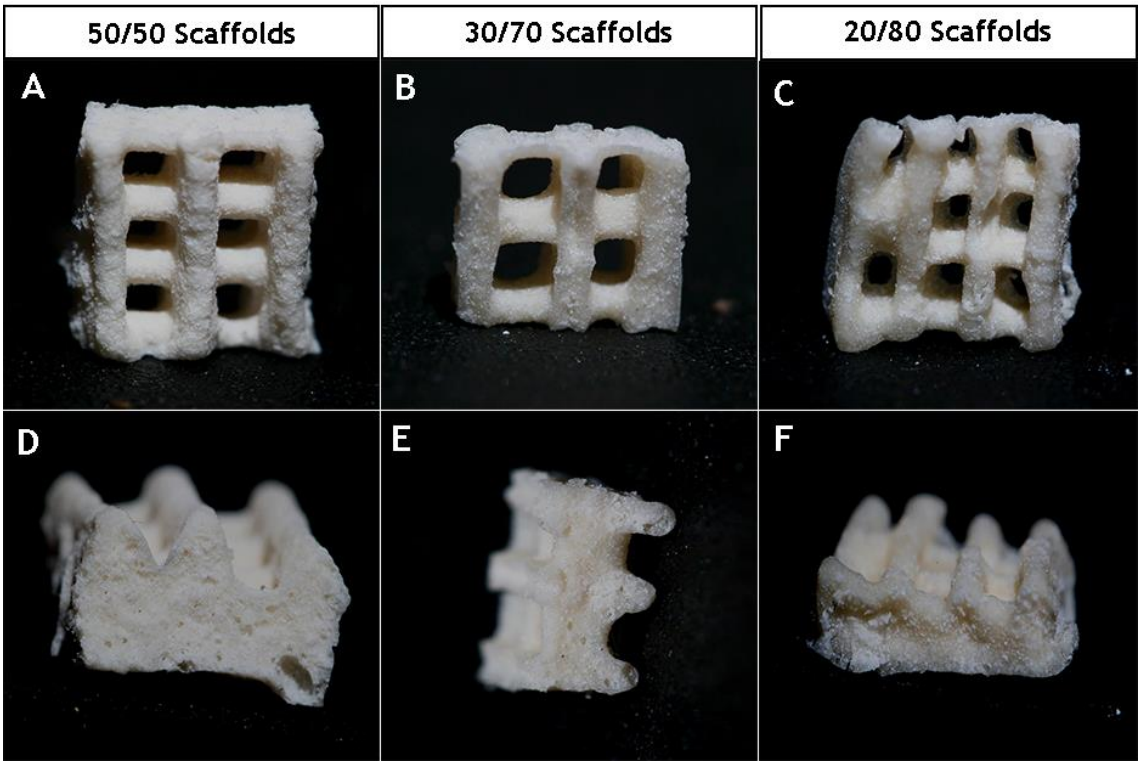

Figure 10 – Images of the different 50/50 (A, D), 30/70 (B, E) and 20/80 (C, F) scaffolds surface.

Afterwards, SEM analysis of the 50/50 scaffolds was performed to characterize their morphology, namely pore size and surface features, Figure 11.

SEM images showed that the scaffolds have a rough surface (Figure 11B). As previously described in the literature, cellular behavior depends largely on the materials surface properties. Surface roughness has a direct influence on cellular morphology, adhesion and proliferation (42). However, cells response to rough surfaces depends on their type (30). Human OB attach more rapidly and synthesize more extracellular matrix in the presence of rough surfaces, than in the presence of smooth surfaces (60). This occurs because cell adhesion to the surface is affected by the enlargement of the cell contact area (33). The contact area increases with increasing surface roughness (33).

Furthermore, rough surfaces are known to affect the material wettability. This influences the material-cell interactions (30, 61). For hydrophilic surfaces, the higher the roughness of the surfaces, the lower is the contact angle, i.e., the surface is more hydrophilic (61). However, for hydrophobic surfaces, higher roughness at the surface, is equivalent to higher contact angles (61). The hydrophilic properties of the rough surfaces contribute for a better cell attachment and fluid diffusion (61).

In addition it is also possible to verify in Figure 11 A,B, that the scaffolds surface is slightly regular. It is emphasized in the literature that the regularity and symmetry of the materials surfaces plays an important role in cellular responses (62).

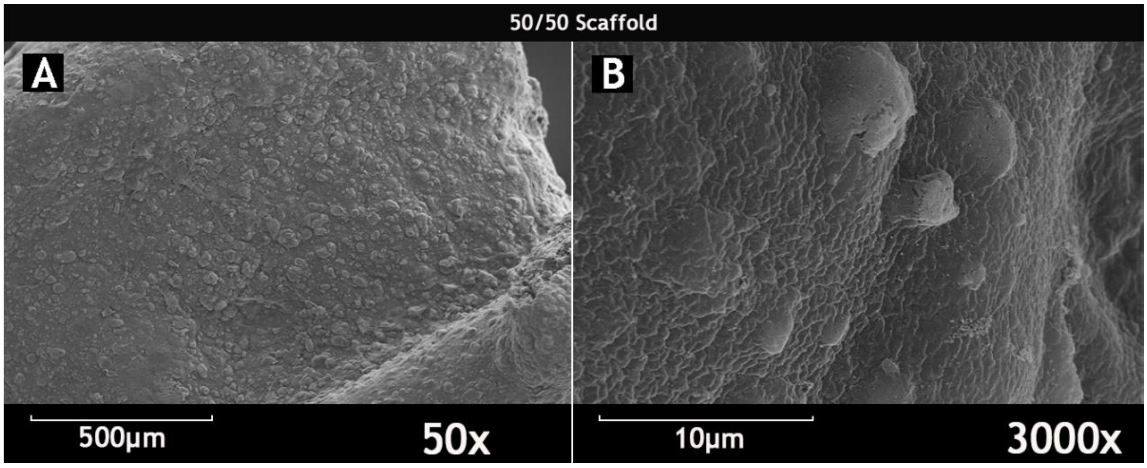

Figure 11 – SEM images of the morphology of 50/50 Scaffolds. Representation of the 50/50 scaffolds at different magnification 50x (A) and 3000x (B).

Subsequently, the pore diameter of the 50/50 and 20/80 scaffolds was studied. According to the literature, the rates of reticulation can influence the structure and shape of the material, namely the pores size (58). Another factor that can affect the pores size is the concentrations of calcium crosslinker cations and polyanionic alginate (41).

The results presented in the SEM images (Figure 12 A,B), show that the pore diameter of scaffolds ranges between 551µm and 875µm, for 20/80 scaffolds and 50/50 scaffolds, respectively. The pore diameter is smaller in the 20/80 scaffolds, which is caused by the higher percentage of alginate. This result may be related to the fact that there are more calcium-alginate connections. In the 50/50 scaffolds, where alginate concentration is lower, the pore size is larger, since there are fewer connections with calcium alginate.

Such results are of crucial importance, since pore diameters ranging from 200µm to 900µm have shown to improve osteoblast-bone deposition and proliferation and also ensuring the nutrients distribution (7).

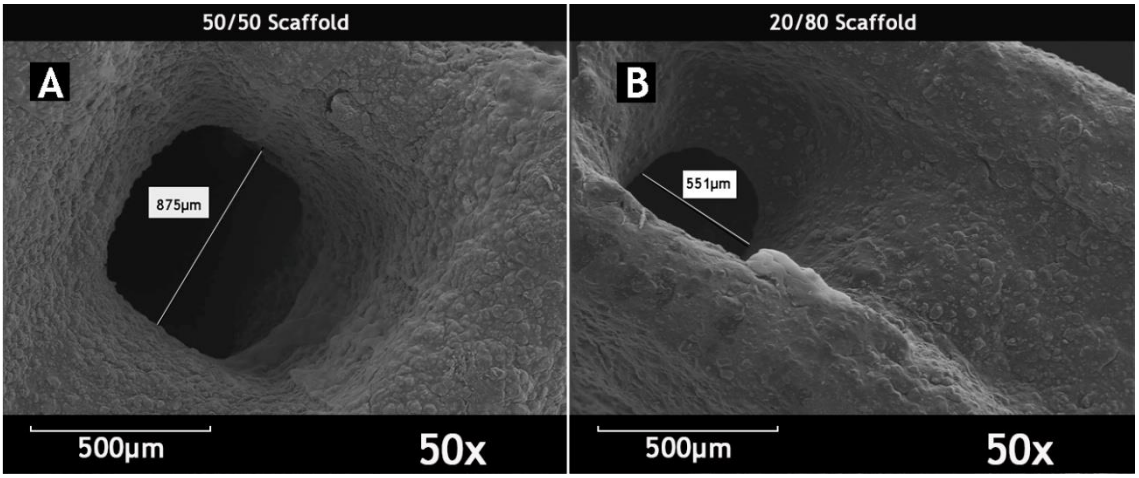

Figure 12 - SEM images of pores sizes of 50/50 scaffolds at 50x (A) and 20/80 scaffolds at 50x (B).

3.2. Physicochemical Characterization

3.2.1. - Fourier Transform Infrared Spectroscopy (FTIR)

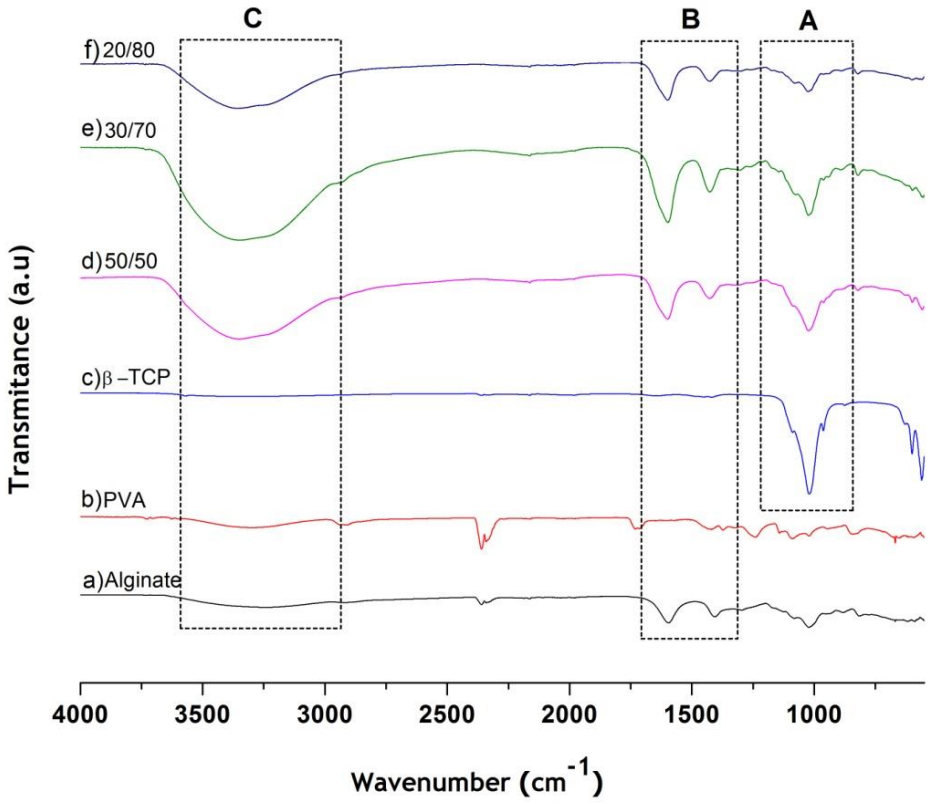

Figure 13 – FTIR analysis of the powders and 3D scaffolds. Alginate (a), PVA (b), ß-TCP (c), 50/50 scaffolds (d), 30/70 scaffolds (e) and 20/80 scaffolds (f).

FTIR analyses were performed in order to evaluate the physicochemical properties of the 50/50, 30/70 and 20/80 samples of the produced scaffolds.

The ß-TCP's FTIR spectra obtained for the powder and for the scaffolds samples revealed a major band at 1020 cm^{-1} (Figure 13, area A), which is typically assigned to the P–O stretching, revealing inorganic phosphate components of ß-TCP (36). No relevant variations were observed between the different ß-TCP's FTIR spectra.

The sodium alginate FTIR spectra for the powder and for the scaffolds revealed peaks at 1600 and 1400 cm^{-1} (Figure 13, area B), which correspond to the C=O stretching of the carboxylic group (63, 64). No relevant variations were observed between the different sodium alginate FTIR spectra obtained for the different sample.

The band observed in alginate and in the scaffolds samples, between 3000-3700 cm^{-1} (Figure 13, area C) belongs to an OH stretch of water. The band has a higher intensity in the spectra corresponding to the scaffolds (65).

3.2.2. X-Ray Diffraction (XRD)

Further analysis of the samples was done by XRD analysis to confirm the presence of crystalline phases of ß-TCP. The Figure 14A shows two intense peaks located at 2Θ=25°-32°. This peaks are characteristic of ß-TCP, as it can also be observed for the commercial ß-TCP spectrum (Figure 14b) (36). These characteristic peaks of the ß-TCP are present in all the manufactured scaffolds, Figure 14 (c,d,e). So, it is important to underline that after all the manufacturing process, the ceramic component of the scaffolds preserved their highly crystalline structure, since no anomalous crystalline phases were identified. The crystallinity is important to the bioactivity of the scaffolds, because it determines the rate of dissolution (66). The ß-TCP dissolution affects bone cells activity, through the release of Ca^{2+} and PO_4^{3-} ions, and by enhancing bone tissue formation rates (66).

FTIR and XRD results are important for the projected application, since the scaffolds maintained their physicochemical properties that are important for promoting cell adhesion, and also bone regeneration.

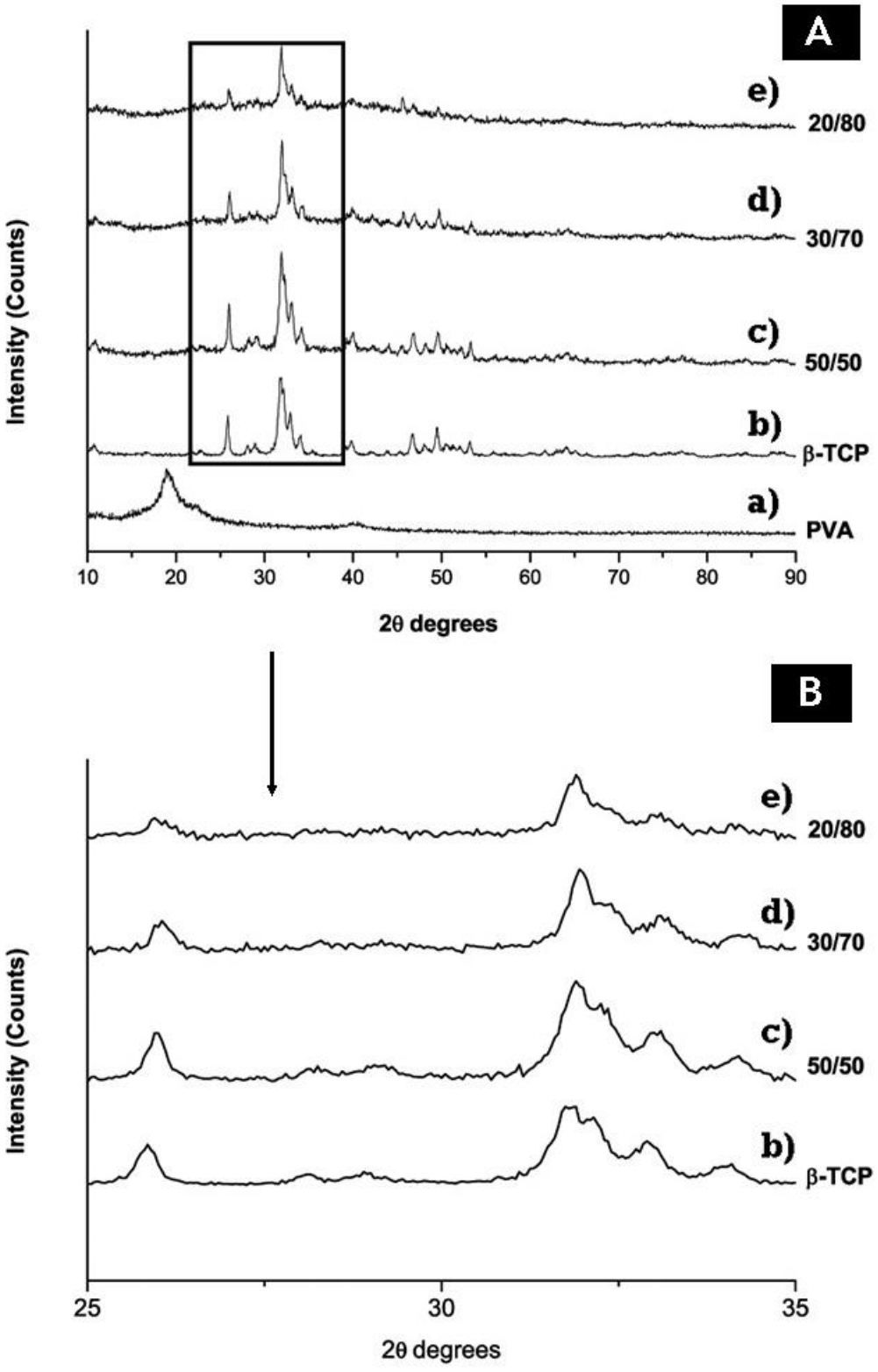

Figure 14- X-Ray spectra of the powders and 3D scaffolds. PVA (a), ß-TCP (b), 50/50 scaffolds (c), 30/70 scaffolds (d) and 20/80 scaffolds (e), (A), and zoomed XRD spectra in a range between 25°-35°, (B).

3.2.3. Energy Dispersive Spectroscopy

An energy dispersive spectroscopic (EDS) analysis of the scaffolds was also performed to characterize the distribution of elemental calcium and phosphorus in the scaffolds. The results show a slight increase in phosphate and calcium ions in the 50/50 scaffold, followed by 30/70 and 20/80, respectively. These results are in agreement with the scaffolds ß-TCP composition.

Table 2 - EDS analysis of the produced 3D scaffolds.

Scaffolds	O	Na	P	Cl	Ca
50/50	61.23%	0.50%	7.69%	11.96%	18.62%
30/70	64.18%	0.80%	5.37%	14.37%	15.27%
20/80	68.45%	1.08%	3.50%	13.93%	13.04%

3.3. Alginate/ß-TCP Composite Scaffolds: Mechanical Characterization.

The mechanical behavior of the 3D scaffolds was characterized by testing the resistance to compression and by determining the Young's modulus tests, Figure 15.

Figure 15 shows that the Young´s modulus and compressive strength of the 50/50 scaffolds are higher than that of the other samples. A suitable scaffold to be used for bone regeneration must have both flexibility and resistance to compression (2). Previous studies have shown that although alginate has several good properties for the application in bone regeneration, when it is used alone it does not have the mechanical properties suitable for this biomedical application. (67) To overcome this problem, its addition to a ceramic material, such as ß-TCP, can enhance the mechanical properties of the produced scaffolds (67). Furthermore, several studies have also reported that one of the main limitations of the use of bioceramics for bone regeneration are related to their mechanical properties, since they are brittleness and have a low fatigue resistance (18, 45). Thus, to improve the mechanical properties of scaffolds, composite systems like bioceramics/polymers can be used (45). Notwithstanding, it is necessary to find a balance between the different materials.

Through the analysis of Figure 15, it is possible to observe that the young´s modulus and compressive strength is higher for the 50/50 scaffolds when compared to the 30/70 and 20/80 scaffolds. With the increase of ß-TCP concentration the Young´s modulus and compressive strength increases, (Figure 15 A,B).

Thus the results are likely correlated with the previously described, the Young´s modulus and compressive strength is greater in the 50/50 scaffolds, since these scaffolds have higher percentage of ß-TCP followed by 30/70 and 20/80 respectively. This result is consistent with a study previously performed by Matsuno *et al*, where ß-TCP was selected to reinforce the initial strength of an alginate hydrogel (67).

Moreover, the mechanical properties of the scaffolds are linked with the biodegradability rate (7). Scaffolds with improved mechanical properties have a slower degradation rate, maintaining their mechanical stability (68). This is important, because, the degradation ratio must be compatible with the ingrowth of the newly formed bone tissue (34). The 50/50 scaffolds have better mechanical properties than the others, which results in a greater mechanical stability, maintaining the spaces required for cell ingrowth and matrix production, during bone formation (7).

Furthermore, comparing the mechanical properties of 50/50 scaffolds with those presented by the natural cancellous bone, it is possible to observe that these scaffolds have less compressive strength and greater young´s modulus (34). This suggests that despite having less compression strength, the properties of the 50/50 scaffolds are improved with the increase in elasticity.

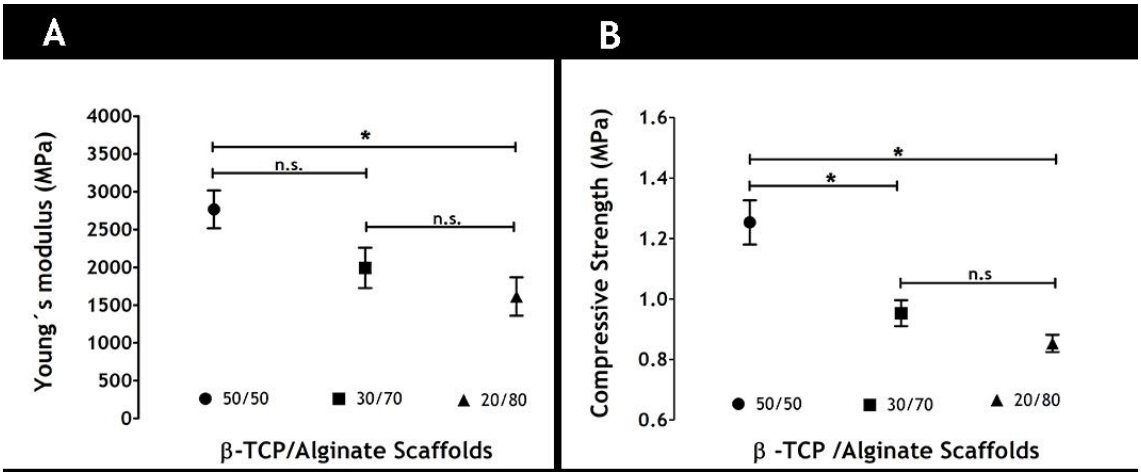

Figure 15 – Characterization of scaffolds mechanical properties. Young's Modulus (A) and Compressive Strength of scaffolds (B). 50/50, 30/70 and 20/80 ß-TCP/Alginate scaffolds. Statistical analysis was performed using one-way ANOVA with Newman-Keuls test (* $p < 0.05$).

3.4. Determination of the Water Contact Angle

Other important physicochemical property that influences the bioactivity and regenerative capacity of a scaffold is their hydrophilic character (30).

The hydrophobic/hydrophilic character of the surface of the 3D structures was characterized by the determination of the contact angles (30). In accordance to what was previously described in several studies, hydrophilic properties of the scaffolds are very important for the uniform attachment of cells and fluid diffusion, that are fundamental for maintaining cell viability (45). Studies performed by Wei *et al*, also reported that the osteoblasts cells adhesion increase when the water contact angle of the material surface decrease (30).

Generally, surfaces are considered hydrophilic when the contact angle ranges between 0º and 30º and mildly hydrophilic when it is between 31º and 90º. Surfaces that show a contact angle higher than 90º are usually considered hydrophobic (69).

Table 3 shows the contact angles obtained for the different scaffolds. The results obtained show that all samples present a moderately hydrophilic character, since the contact angle is around 70º. Such suggests that the combined materials are moderately hydrophilic which is supported by what is already described in the literature (58). These hydrophilic character of the produced scaffolds is mostly a consequence of the high carboxyl and hydroxyl groups present in alginate (26).

Studies performed by Valente *et al.*, reported that hydrophilic scaffolds allow cell adhesion and differentiation as well as infiltration of oxygen and nutrients from body fluids into the scaffolds, which have an essential role for the successful repair of bone defects (70).

Table 3- Contact Angles of the produced scaffolds.

Scaffolds (β-TCP/Alginate)	Water Contact Angle
50/50	**70.7º ± 4.4º**
30/70	**70.3º ± 4.5º**
20/80	**70.3º ± 4.1º**

3.5. Determination of the Total Porosity of Scaffolds

To evaluate the total porosity of the scaffolds, liquid displacement method using ethanol was performed (57). One of the important requirements for the production of scaffolds used in bone tissue regeneration is to achieve an equilibrium between scaffolds porosity and their

mechanical properties (7). The porosity influences both the mechanical and biological properties of the scaffolds (71).

From the analysis of Figure 16, it is possible to observe that the 50/50 scaffolds present the higher value of porosity (52 %), when compared to the 30/70 (46 %) and 20/80 (23 %) scaffolds.

According to what was previously described by Santos et al., this porosity results can be related with the density of the scaffolds (36). Possibly, due to the fact that porosity and density are inversely proportional. Furthermore, the processing of powder materials originated structures with an associated microporosity as a result of the voids formed between the powder particles (36). 50/50 scaffolds have more β-TCP and subsequently a higher degree of microporosity, as presented above in the Macroscopic images (Figure 10 D), resulting in a higher porosity. In conclusion, 50/50 scaffolds allow better cell migration, adhesion and proliferation and also facilitate the transport of oxygen and nutrients.

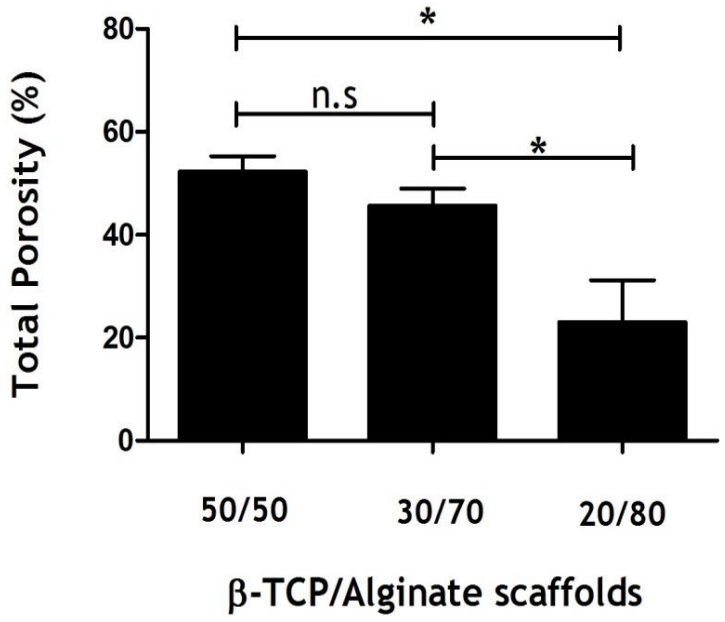

Figure 16 – Total porosity of scaffolds. Statistical analysis was performed using one-way ANOVA with Newman-Keuls test (* $p < 0.05$).

3.6. Analysis of the Biological Properties of the Scaffolds

3.6.1. Characterization of the Cytotoxic Profile of the Scaffolds

In order to characterize the cytocompatibility of the ß-TCP/Alginate scaffolds, *in vitro* studies were performed. For this purpose, human osteoblasts cells were cultured in the presence of 3D scaffolds for up to 7 days and their biocompatibility evaluated at the indicated time points. Cell adhesion and proliferation in the presence of the scaffolds were characterized by using an inverted light microscope (Figure 17) and SEM analysis (Figure 18).

The optical microscopy images acquired 1 and 7 days after cell seeding showed that cells adhered and proliferate, in the presence of the ß-TCP/Alginate scaffolds, (Figure 17 A to F). The results are similar for the negative control, (Figure 17 G to H). Regarding the positive control, no cell adhesion or proliferation was observed. Dead cells with their typical spherical shape can be observed in Figure 17 (I to J).

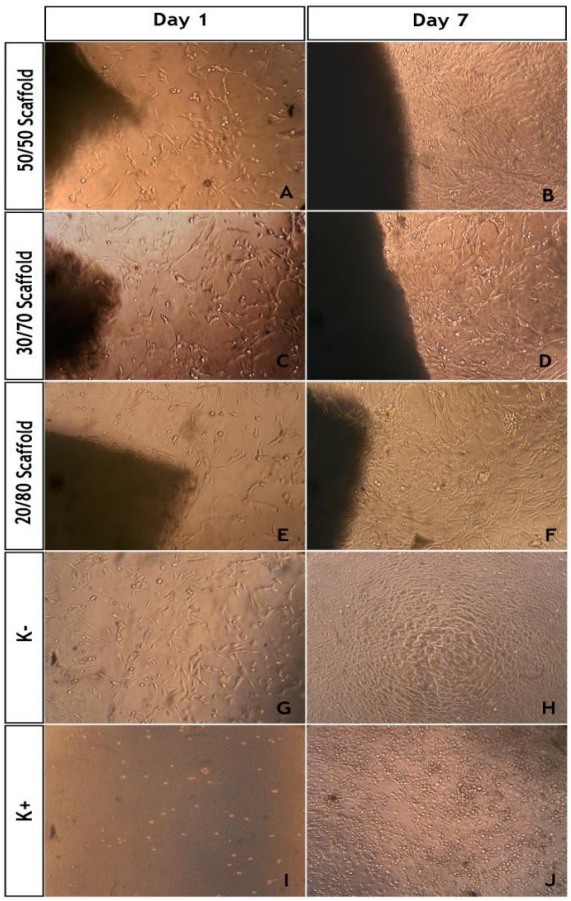

Figure 17- Macroscopic images of human osteoblasts cells in the presence of scaffolds, 1 and 7 days after seeding 50/50 scaffolds (A,B) 30/70 scaffolds (C,D) 20/80 scaffolds (E,F) negative control (K-) (G,H) and positive control (K+) (I,J).

SEM analysis was performed to characterize cellular adhesion both on the surface and inside the scaffolds.

As previously described in section 3.1, SEM images revealed that scaffolds had a slightly regular surface, high level of roughness and porosity, which contribute for osteoblasts adhesion and proliferation as well as for nutrients diffusion into the scaffold.

SEM images show that cells adhered and grew within the ß-TCP/Alginate scaffolds after 1 day of being in the presence of the scaffold, Figure 18 (A,C,E).

To evaluate if cells remained viable and that cell proliferation occurred through time, SEM images were also acquired after 7 days. This SEM images also allowed the visualization of cells attached and spread on the surface of ß-TCP/Alginate scaffolds, (Figure 18 B,D,F).

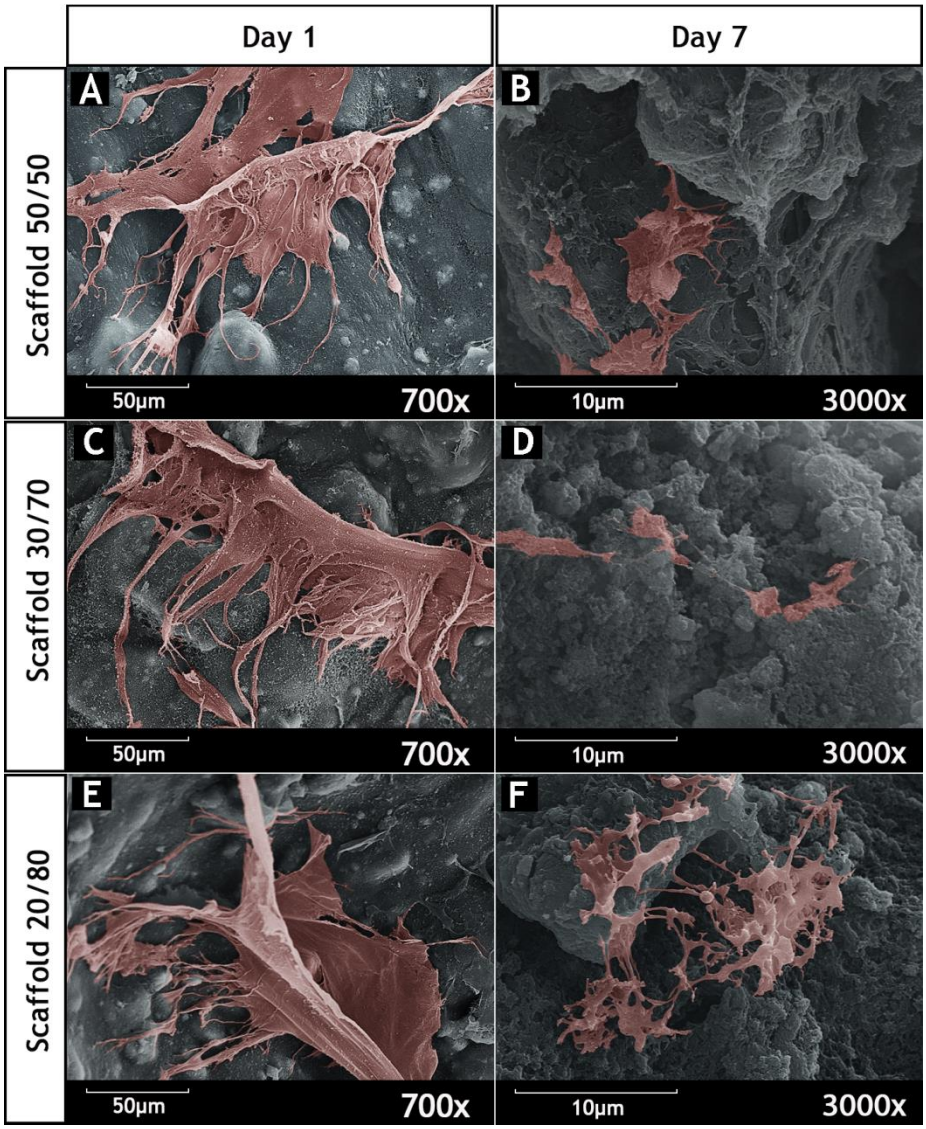

Figure 18 – SEM micrographs of osteoblasts morphology in the presence of the different ß-TCP/Alginate scaffolds. 50/50 scaffolds (A,B), 30/70 scaffolds (C,D) and 20/80 scaffolds (E,F).

Moreover, the *in vitro* cytotoxicity was also evaluated by an MTS assay. This assay showed a significant difference between cells in presence of ß-TCP/Alginate and in the positive control ($p<0.05$) after 1 and 7 days of incubation, suggesting that the scaffolds did not affect cell viability (Figure 19). The MTS assay also showed a significant difference in the 50/50 and 20/80 scaffolds between the first and seventh day ($p<0.05$). The 30/70 scaffold did not present significant difference within this period of time.

It is also possible to observe that cell viability is higher for the 50/50 scaffolds, i.e., with the increase of ß-TCP, an increase in cell viability was observed, Figure 19.

The results are supported by results obtained by Fuji *et al.*, which report that the apatite formation through ß-TCP dissolution at physiological conditions, affect the osteoblasts behavior (53). The presence of Ca^{+} and PO_4^{3-} resultant of ß-TCP dissolution is important for the osteoconduction and osteoinduction process, providing a favorable environment for osteoblast attachment and growth.

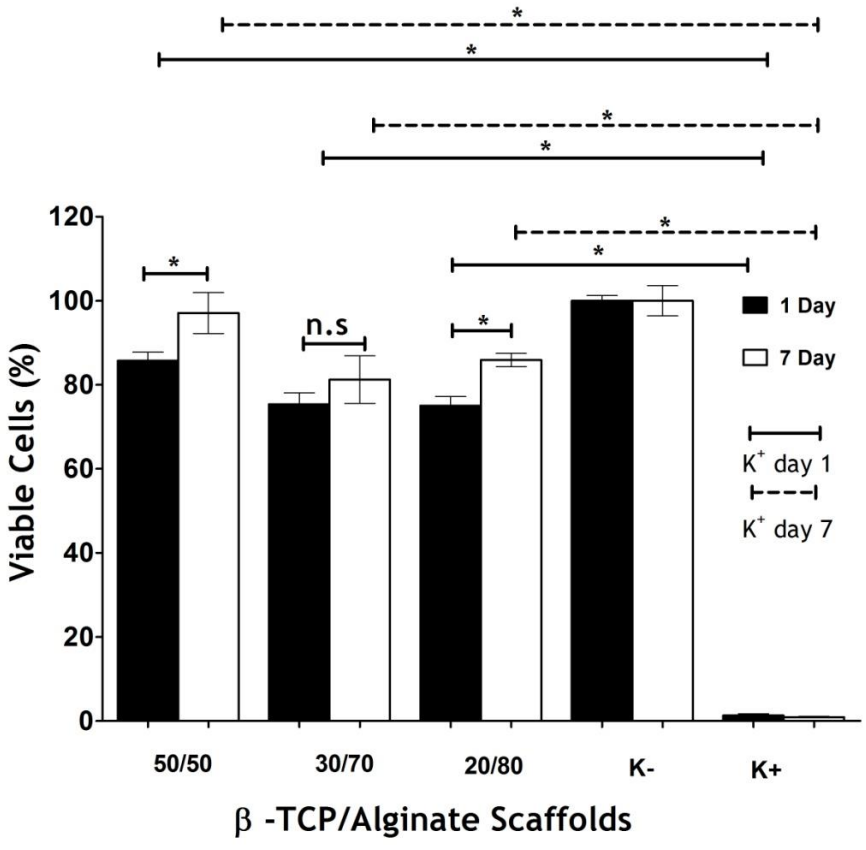

Figure 19 – Evaluation of human osteoblast cell viability when cultured in the presence of different ß-TCP/Alginate scaffolds. Cultures were evaluated for 1 and 7 days. (K+) positive control and (K-) negative control, indicate dead and viable cells, respectively. Each result is the mean ± standard error of the mean of at least three independent experiments. Statistical analysis was performed using one-way ANOVA with Dunnet's post hoc test (* $p < 0.05$).

These results are further confirmed by CLSM analysis, 4 days after osteoblasts being in contact with 50/50 scaffolds.

As shown in Figure 20 A, during osteoblasts contact with scaffolds, it is readily visible that cells were able to adhere and proliferate in the 50/50 scaffolds formulation, further highlighting its biocompatibility and appropriated physicochemical properties for bone regenerative medicine (Figure 20 A).

In Figure 20 B it is possible to observe the 3D reconstruction and depth analysis of the 50/50 scaffold, up to 200 µm. This shows that osteoblasts are capable of migrating and attaching into deep sections of the scaffolds. Some cells were localized up to 200 µm within the scaffolds architecture (Figure 20 B).

This is an interest result, since the deposition of bone matrix inside the scaffold will eventually fill the bone defect while the scaffold is biodegraded, ultimately leading to the establishment of the original structure and function of the native bone.

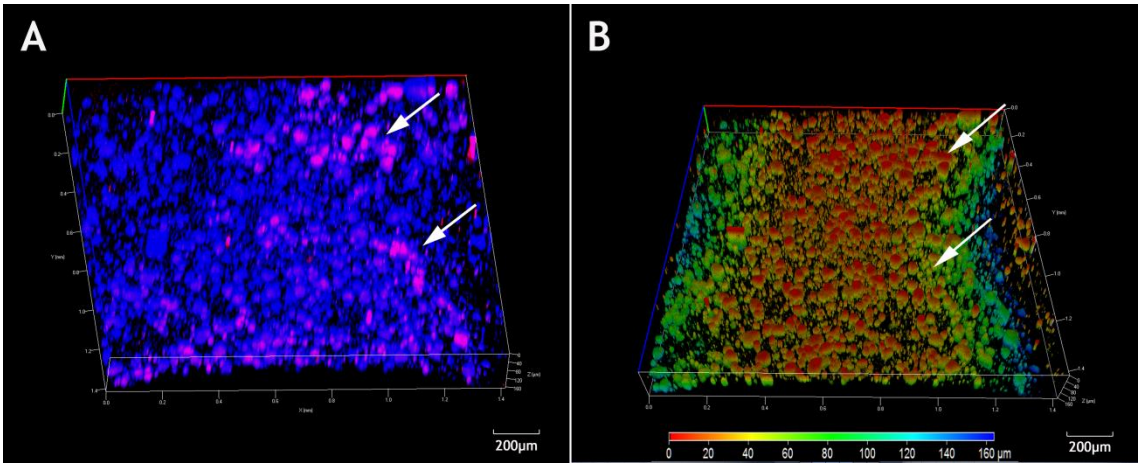

Figure 20 – CSLM images of osteoblasts in contact with the 50/50 scaffold. 3D reconstruction of the 50/50 scaffold seeded with osteoblasts after 4 days in culture. Blue channel: 50/50 scaffold; Red Channel: PI stained nucleus of osteoblasts (A), Depth coding analysis of osteoblasts distribution within the 3D volume of the scaffold (B).

Chapter IV – Conclusions and Future Perspectives

4. Conclusions and Future Perspectives

Bone defects have been increasing, affecting millions of people worldwide. Temporary and biodegradable scaffolds are a good choice to overcome this problem. Nowadays, several techniques are used for the production of scaffolds. Rapid prototyping technologies allow the construction of 3D models with a well-defined structure and porosity, presenting some advantages over conventional techniques. Fab@home model is one of the newer printers used for production of 3D structures to be used in bone tissue regeneration. However, further studies must be performed in order to increase the suitability of this equipment for this particular biomedical application. In this study ß-TCP/Alginate scaffolds were produced by rapid prototyping using a Fab@home model. Three different groups of scaffolds were produced, varying the ratios between the concentrations of ß-TCP and Alginate. Respectively, 50/50 % (w/w), 30/70 % (w/w) and 20/80 % (w/w), ß-TCP/Alginate scaffolds.

The physicochemical results (FTIR, XRD and EDS) showed, that after all the manufacturing process all samples have a highly crystalline structure and contain in their composition calcium and phosphate elements. The produced scaffolds are porous structures with hydrophilic character, which allows an improved cell adhesion and fluid diffusion within scaffolds. SEM images show that scaffolds present a rough surface. The *in vitro* cytotoxic assays performed show a good cell-scaffold interaction and biocompatibility, enhanced in the 50/50 scaffolds. Confocal scanning laser microscopy shows the osteoblasts distribution within the 50/50 scaffolds 4 days after osteoblasts be in the presence of scaffolds.

It is possible to conclude that the 50/50 scaffolds present better mechanical and biological properties than the 30/70 and 20/80 scaffolds, respectively. The results suggest that the scaffolds with higher ß-TCP percentage have better conditions for the osteogenic process and better mechanical properties than the ones with higher alginate polymer percentage. Mechanical properties results show that 50/50 scaffolds have more compressive strength and also Young´s modulus.

In a near future, an enhancement of the mechanical properties would be to optimize the pore size, in order to improve the mechanical resistance of the scaffolds. Another approach would be the addition of a ceramic compound such as hydroxyapatite for improving the mechanical resistance. So, the scaffold will maintain their bioactive property but with a better resistance. Furthermore, methodologies like the application of a coating of a resistant material, through techniques such as electro-spinning, can possible be used to improve the mechanical properties of the produced scaffolds.

Chapter V – Bibliography

1. Ralston SH. Structure and metabolism of bone. Medicine. 2005;33(12):58-60.

2. Seeley RR, Stephens TD, Tate P. Anatomia & Fisiologia. 8th ed: Lusociência-Edições Técnicas e Científicas, Lda.; 2008.

3. Van De Graaff KM. Human Anatomy. 6th ed: The McGraw-Hill Companies, Inc.; 2002.

4. Marieb EN, Hoehn K. Human Anatomy & Physiology. 7th ed: Pearson Education, Inc.; 2007.

5. Alvarez K, Nakajima H. Metallic scaffolds for bone regeneration. Materials. 2009;2(3):790-832.

6. Hsiong SX, Mooney DJ. Regeneration of vascularized bone. Periodontology 2000. 2006;41(1):109-22.

7. Salgado AJ, Coutinho OP, Reis RL. Bone tissue engineering: state of the art and future trends. Macromolecular bioscience. 2004;4(8):743-65.

8. Mackie E. Osteoblasts: novel roles in orchestration of skeletal architecture. The international journal of biochemistry & cell biology. 2003;35(9):1301-5.

9. Neve A, Corrado A, Cantatore FP. Osteoblast physiology in normal and pathological conditions. Cell and tissue research. 2011;343(2):289-302.

10. Mebarek S, Abousalham A, Magne D, Do LD, Bandorowicz-Pikula J, Pikula S, et al. Phospholipases of mineralization competent cells and matrix vesicles: roles in physiological and pathological mineralizations. International journal of molecular sciences. 2013;14(3):5036-129.

11. Jayakumar P, Di Silvio L. Osteoblasts in bone tissue engineering. Proceedings of the institution of mechanical engineers, Part H: journal of engineering in medicine. 2010;224(12):1415-40.

12. Clarke B. Normal bone anatomy and physiology. Clinical journal of the american society of nephrology. 2008;3(Supplement 3):S131-S9.

13. Jang J, Castano O, Kim H. Electrospun materials as potential platforms for bone tissue engineering. Advanced drug delivery reviews. 2009;61(12):1065-83.

14. Hadjidakis DJ, Androulakis II. Bone remodeling. Annals of the new york academy of sciences. 2006;1092(1):385-96.

15. Robling AG, Castillo AB, Turner CH. Biomechanical and molecular regulation of bone remodeling. Annual review of biomedical engineering 2006;8(1):455-98.

16. Raisz LG. Physiology and pathophysiology of bone remodeling. Clinical chemistry. 1999;45(8):1353-8.

17. Chai YC, Carlier A, Bolander J, Roberts SJ, Geris L, Schrooten J, et al. Current views on calcium phosphate osteogenicity and the translation into effective bone regeneration strategies. Acta biomaterialia. 2012;8(11):3876–87.

18. Chiara G, Letizia F, Lorenzo F, Edoardo S, Diego S, Stefano S, et al. Nanostructured biomaterials for tissue engineered bone tissue reconstruction. International journal of molecular sciences. 2012;13(1):737-57.

19. Williams DF. To engineer is to create: the link between engineering and regeneration. Trends in biotechnology. 2006;24(1):4-8.

20. Djouad F, Guerit D, Marie M, Toupet K, Jorgensen C, Noel D. Mesenchymal Stem Cells: New insights into bone regenerative applications. Journal of biomaterials and tissue engineering. 2012;2(1):14-28.

21. Hutmacher DW, Sittinger M, Risbud MV. Scaffold-based tissue engineering: rationale for computer-aided design and solid free-form fabrication systems. Trends in biotechnology. 2004;22(7):354-62.

22. Kneser U, Schaefer D, Polykandriotis E, Horch R. Tissue engineering of bone: the reconstructive surgeon's point of view. Journal of cellular and molecular medicine. 2006;10(1):7-19.

23. Giannoudis PV, Dinopoulos H, Tsiridis E. Bone substitutes: an update. Injury. 2005;36(3):S20-S7.

24. Hutmacher DW. Scaffold design and fabrication technologies for engineering tissues—state of the art and future perspectives. Journal of biomaterials science, polymer edition. 2001;12(1):107-24.

25. Bhat S, Kumar A. Biomaterials and bioengineering tomorrow's healthcare. Biomatter. 2013;3(2):e24717.

26. Valente J, Valente T, Alves P, Ferreira P, Silva A, Correia I. Alginate based scaffolds for bone tissue engineering. Materials science and engineering: C. 2012;32:2596–603.

27. Dreifke MB, Ebraheim NA, Jayasuriya AC. Investigation of potential injectable polymeric biomaterials for bone regeneration. Journal of biomedical materials research part A. 2013;0.

28. Leong K, Cheah C, Chua C. Solid freeform fabrication of three-dimensional scaffolds for engineering replacement tissues and organs. Biomaterials. 2003;24(13):2363-78.

29. Williams DF. On the mechanisms of biocompatibility. Biomaterials. 2008;29(20):2941-53.

30. Chang H, Wang Y. Cell responses to surface and architecture of tissue engineering scaffolds. Regenerative medicine and tissue engineering—cells and biomaterials, InTech:2011;569-88.

31. Hollister SJ. Porous scaffold design for tissue engineering. Nature materials. 2005;4(7):518-24.

32. Dhandayuthapani B, Yoshida Y, Maekawa T, Kumar DS. Polymeric scaffolds in tissue engineering application: a review. International journal of polymer science. 2011;2011:1-19.

33. Yoon H, Kim GH, Koh YH. A Micro-scale surface-structured PCL scaffold fabricated by a 3D plotter and a chemical blowing agent. Journal of biomaterials science, polymer edition. 2010;21(2):159-70.

34. Hutmacher DW, Schantz JT, Lam CXF, Tan KC, Lim TC. State of the art and future directions of scaffold-based bone engineering from a biomaterials perspective. Journal of tissue engineering and regenerative medicine. 2007;1(4):245-60.

35. Suzuki T, Yamamoto T, Toriyama M, Nishizawa K, Yokogawa Y, Mucalo MR, et al. Surface instability of calcium phosphate ceramics in tissue culture medium and the effect on adhesion and growth of anchorage-dependent animal cells. Journal of biomedical materials research. 1997;34(4):507-17.

36. Santos CF, Silva AP, Lopes L, Pires I, Correia IJ. Design and production of sintered ß-tricalcium phosphate 3D scaffolds for bone tissue regeneration. Materials science and engineering: C. 2012;32(5):1293-8.

37. Li X, Bian W, Li D, Lian Q, Jin Z. Fabrication of porous beta-tricalcium phosphate with microchannel and customized geometry based on gel-casting and rapid prototyping. Proceedings of the institution of mechanical engineers, Part H: journal of engineering in medicine. 2011;225(3):315-23.

38. Yang Y, Bumgardner J, Cavin R, Carnes D, Ong J. Osteoblast precursor cell attachment on heat-treated calcium phosphate coatings. Journal of dental research. 2003;82(6):449-53.

39. Christensena BE. Alginates as biomaterials in tissue engineering. Carbohydrate chemistry: chemical and biological approaches. 2011;37:227-58.

40. LeRoux MA, Guilak F, Setton LA. Compressive and shear properties of alginate gel: effects of sodium ions and alginate concentration. Journal of biomedical materials research. 1999;47(1):46-53.

41. Daemi H, Barikani M. Synthesis and characterization of calcium alginate nanoparticles, sodium homopolymannuronate salt and its calcium nanoparticles. Scientia iranica. 2012;19(6):2023–8.

42. Lantada AD, Morgado PL. Rapid Prototyping for biomedical engineering: current capabilities and challenges. Annual review of biomedical engineering. 2012;14:73-96.

43. Seitz H, Rieder W, Irsen S, Leukers B, Tille C. Three-dimensional printing of porous ceramic scaffolds for bone tissue engineering. Journal of biomedical materials research Part B: applied biomaterials. 2005;74(2):782-8.

44. Nandakumar A, Barradas A, de Boer J, Moroni L, van Blitterswijk C, Habibovic P. Combining technologies to create bioactive hybrid scaffolds for bone tissue engineering. Biomatter. 2013;3(1):1-13.

45. Yeo MG, Kim GH. Preparation and characterization of 3D composite scaffolds based on rapid-prototyped PCL/ß-TCP struts and electrospun PCL coated with collagen and HA for bone regeneration. Chemistry of materials. 2011;24(5):903-13.

46. Stevens B, Yang Y, Mohandas A, Stucker B, Nguyen KT. A review of materials, fabrication methods, and strategies used to enhance bone regeneration in engineered bone tissues. Journal of biomedical materials research Part B: applied biomaterials. 2008;85(2):573-82.

47. Ang T, Sultana F, Hutmacher D, Wong YS, Fuh J, Mo X, et al. Fabrication of 3D chitosan–hydroxyapatite scaffolds using a robotic dispensing system. Materials science and engineering: C. 2002;20(1):35-42.

48. Wüst S, Müller R, Hofmann S. Controlled positioning of cells in biomaterials—approaches towards 3D tissue printing. Journal of functional biomaterials. 2011;2(3):119-54.

49. Lixandrão Filho A, Cheung P, Noritomi P, da Silva J, Colangelo N, Kang H, et al. Construction and adaptation of an open source rapid prototyping machine for biomedical research purposes-a multinational collaborative development. Innovative developments in design and manufacturing. 2009:469-73.

50. Kang K, Hockaday L, Butcher J. Quantitative optimization of solid freeform deposition of aqueous hydrogels. Biofabrication. 2013;5(3):1-13.

51. Cohen DL, Lo W, Tsavaris A, Peng D, Lipson H, Bonassar LJ. Increased mixing improves hydrogel homogeneity and quality of three-dimensional printed constructs. Tissue engineering Part C: methods. 2010;17(2):239-48.

52. Vivanco J, Aiyangar A, Araneda A, Ploeg H-L. Mechanical characterization of injection-molded macro porous bioceramic bone scaffolds. Journal of the mechanical behavior of biomedical materials. 2012;9:137-52.

53. Fuji T, Anada T, Honda Y, Shiwaku Y, Koike H, Kamakura S, et al. Octacalcium Phosphate–Precipitated Alginate Scaffold for Bone Regeneration. Tissue engineering Part A. 2009;15(11):3525-35.

54. Wu X, Liu Y, Li X, Wen P, Zhang Y, Long Y, et al. Preparation of aligned porous gelatin scaffolds by unidirectional freeze-drying method. Acta biomaterialia. 2010;6(3):1167-77.

55. Lacroix D, Chateau A, Ginebra M-P, Planell JA. Micro-finite element models of bone tissue-engineering scaffolds. Biomaterials. 2006;27(30):5326-34.

56. Correia TR, Antunes BP, Castilho PH, Nunes JC, Pessoa de Amorim MT, Escobar IC, et al. A bi-layer electrospun nanofiber membrane for plasmid DNA recovery from fermentation broths. Separation and purification technology. 2013;112:20-5.

57. Nie H-L, Zhu L-M. Adsorption of papain with Cibacron Blue F3GA carrying chitosan-coated nylon affinity membranes. International journal of biological macromolecules. 2007;40(3):261-7.

58. Cho SH, Lim SM, Han DK, Yuk SH, Im GI, Lee JH. Time-dependent alginate/polyvinyl alcohol hydrogels as injectable cell carriers. Journal of biomaterials science, polymer edition. 2009;20(7-8):863-76.

59. Karageorgiou V, Kaplan D. Porosity of 3D biomaterial scaffolds and osteogenesis. Biomaterials. 2005;26(27):5474-91.

60. Dos Santos E, Farina M, Soares G, Anselme K. Chemical and topographical influence of hydroxyapatite and ß-tricalcium phosphate surfaces on human osteoblastic cell behavior. Journal of biomedical materials research Part A. 2009;89(2):510-20.

61. Navarro M, Aparicio C, Charles-Harris M, Ginebra M, Engel E, Planell J. Development of a biodegradable composite scaffold for bone tissue engineering: physicochemical, topographical, mechanical, degradation, and biological properties. Ordered polymeric nanostructures at surfaces. 200: Springer; 2006:209-31.

62. Lenhert S, Meier M-B, Meyer U, Chi L, Wiesmann HP. Osteoblast alignment, elongation and migration on grooved polystyrene surfaces patterned by Langmuir–Blodgett lithography. Biomaterials. 2005;26(5):563-70.

63. Pathak TS, San Kim J, Lee S-J, Baek D-J, Paeng K-J. Preparation of alginic acid and metal alginate from algae and their comparative study. Journal of polymers and the environment. 2008;16(3):198-204.

64. Lawrie G, Keen I, Drew B, Chandler-Temple A, Rintoul L, Fredericks P, et al. Interactions between alginate and chitosan biopolymers characterized using FTIR and XPS. Biomacromolecules. 2007;8(8):2533-41.

65. Lambert JB, Shurvell HF, Lightner DA, Cooks RG. Organic structural spectroscopy.: Prentice Hall; 1998.

66. Berube P, Yang Y, Carnes DL, Stover RE, Boland EJ, Ong JL. The effect of sputtered calcium phosphate coatings of different crystallinity on osteoblast differentiation. Journal of periodontology. 2005;76(10):1697-709.

67. Matsuno T, Hashimoto Y, Adachi S, Omata K, Yoshitaka Y, Ozeki Y, et al. Preparation of injectable 3D-formed. BETA.-tricalcium phosphate bead/alginate composite for bone tissue engineering. Dental materials journal. 2008;27(6):827-34.

68. Ghanaati S, Barbeck M, Detsch R, Deisinger U, Hilbig U, Rausch V, et al. The chemical composition of synthetic bone substitutes influences tissue reactions in vivo: histological and histomorphometrical analysis of the cellular inflammatory response to hydroxyapatite, beta-tricalcium phosphate and biphasic calcium phosphate ceramics. Biomedical materials. 2012;7(1):015005.

69. Shalumon K, Anulekha K, Chennazhi K, Tamura H, Nair S, Jayakumar R. Fabrication of chitosan/poly (caprolactone) nanofibrous scaffold for bone and skin tissue engineering. International journal of biological macromolecules. 2011;48(4):571-6.

70. Wang C, Meng G, Zhang L, Xiong Z, Liu J. Physical properties and biocompatibility of a core-sheath structure composite scaffold for bone tissue engineering in vitro. BioMed Research International. 2012;2012.

71. Tarafder S, Balla VK, Davies NM, Bandyopadhyay A, Bose S. Microwave-sintered 3D printed tricalcium phosphate scaffolds for bone tissue engineering. Journal of tissue engineering and regenerative medicine. 2012.